SATELLITE LASER RANGING WORK AT SHANGHAI OBSERVATORY

Satellite Laser Ranging Group

Shanghai Observatory, Academia Sinica

Shanghai, China

1. The First-generation Ruby Laser System

The satellite laser ranging work at the Shanghai Observatory(SO) is one of the topics of the astro-geodynamics research program of the Observatory. We began the development of the first-generation satellite laser ranging system in 1972 in collaboration with the Shanghai Institute of Optics and Fine Mechanics(SIOM). A dye-cell Q-switch ruby laser which produced 2.5 joules in 25-nsec duration time (half-power, full width) with 30 ppm repetition rate was adopted. The aperture of the receiving telescope was 30cm. Because of the poor pointing accuracy of the old alt-az mount, the visual tracking mode only could be used. Table 1 lists the performance of the ruby system. The first echoes from BE-C were received in November 1973. The system was installed at Zô-Sè section of the Shanghai Observatory in the autumn of 1975, which is in the southwest suburb of Shanghai and the coordinates of the laser system are as follows: $\lambda=121^{\circ}\,11'\,19''.63E$ $\varphi=31^{\circ}\,05'\,46''.86$ h=118.3 m.

The system has been in operation since December of the same year, four satellites, BE-C, GEOS-1, GEOS-2 and GEOS-3, have been tracked. The maximum ranges were over 2700km and the accuracy of ranges was about 1-2 meters[1].

2. Prediction of Satellite and Work for the Chinese Ranging Network

The prediction of the satellites(BE-C and GEOS-1) were provided by Purple Mountain Observatory in Nanjing during the early years. Since 1975, we have done the predictions independently. Because we did not participate in any international cooperation at that time and had no new orbital elements of the laser satellites, a method for acquiring the tracks of satellite was developed. By the method, we can in a short time, acquire the tracks of some laser satellites such as GEOS-2, GEOS-3 and LAGEOS at a single station, based only on the previous orbital elements or the observation data collected from references about 1-2 years ago[2].

Five more first-generation ruby ranging systems have been gradually set up in China since 1977. Three of them are at the Beijing Observatory(operation in 1977), the Yunnan Observatory(operation in 1978) and the Guangzhou Satellite Observation Station(operation in 1981). The above three stations and ours all belong to the Academia Sinica. The other two systems, just the same as Guangzhou's, which are in operation in 1980-1981, belong to the geodesy departments. The five systems all use a Pockels cell for a Q-switch and operate at 30 pulses per minute. The lasers generate an output of 1.5 joules in 20-nsec pulse. The resolution of the counters is 6.7-nsec. The apertures of the receiving telescopes are 40-50cm. The visual tracking mode is still adopted, but because of better mounts the percentage of hits typically is 40-60 %.

Now a laser ranging network which consists of the

above-mentioned six stations has been run for a common project organized by the Shanghai Observatory. The first goal of the project is to determine the chord lengthes between the laser stations. The satellites tracked by the network are: GEOS-3, GEOS-1 and BE-C, and no station has the ability to track LAGEOS yet. The predictions of these satellites for the network have been provided routinely by our observatory, the preprocessings of all laser range data obtained by the six stations and reductions of the chord lengthes are being done by our observatory also. For lack of enough range data, no result of the chord lengthes has been got yet.

3. Experimental Nd:YAG Ranging System

In order to participate in the MERIT short campaign (August 1st to October 31st,1980), a great deal of improvements have been made to our ruby system since April 1980 in collaboration with SIOM again, and a decimeter accuracy Nd:YAG experimental laser ranging system was set up.[3] Fig.1 is the block diagram of the Nd:YAG system, the instruments in the figure marked SO were made by our observatory, and the laser and its power supply were made by SIOM. Table 1 lists the main charateristics of the system. The instruments and devices in the laser ranging system were all made in China except a discriminator(Ortec 473A). The Nd:YAG laser consists of an oscillator, an amplifier and a frequency doubler. The oscilator has a transmission coupling unstable plano-convex cavity with an electro-optic Q-switch, the structure being quite simple and compact. The width of the output pulse is about 4-5 nsec, the divergence is about 0.5 mrad and the center of the near field pattern is solid. The energy of output is 80-100 mj in 5320Å. The laser was installed on the top of the telescope tube, and rotated with it. Experiments showed that the output energy did not decrease when the laser had been operated for a month, no ad-

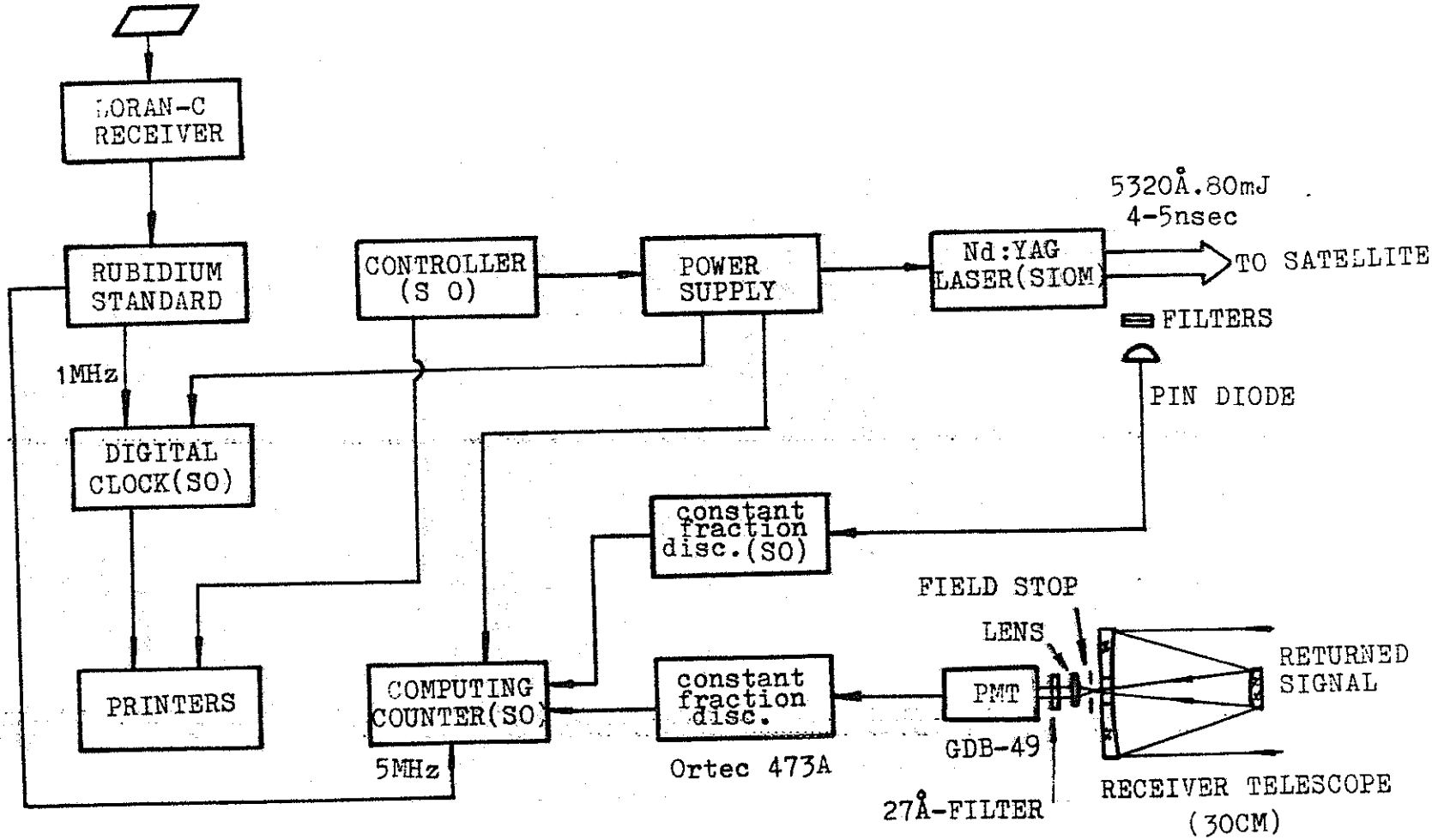

FIG.1 BLOCK DIAGRAM OF Nd:YAG EXPERIMENTAL RANGING SYSTEM

justment was needed.

The photoreceiver and data recording parts consist of a fast photomultiplier, two constant fraction discriminators, a computing counter, a controller, a digital clock and two printers, etc. A Si-pin photodiode which risetime is less than 1-nsec is used for sampling the transmitting pulse attenuated by the filters. A photomultiplier(Type GDB-49) which has a K-Cs-Sb cathode and twelve dynodes is chosen for detecting the returned signals. The PMT has a gain of 3×10^7 and a risetime of 1.9-nsec. In order to improve the accuracy of the measurement of the flight time, a new time interval counter or so-called computing counter was made by ourselves in collaboration with the Shanghai Electronic Instrument Factory, which was designed according to the analogue interpolation method, so that the main frequency is 10 MHz and the resolution is 0.1-nsec. It is shown in the experiment that the performance of the counter is good. Considering the returned signals fluctuating over a wide range in amplitude, we use the constant fraction discriminators to replace the fixed threshold discriminators adopted in the old ruby system for reducing the errors of pulse position measurement. The Model 473A(Ortec) constant fraction discriminator with 100:1 dynamic range is chosen for the receiving channel, and another one made by ourselves is for the transmitting channel which is simpler than commercial products. A lower-level discrimination circuit is designed to estimate and to prevent the noise of the ranging system. The time jitter of the discriminator is less than 0.5-nsec for 4-5 nsec pulse with 40:1 dynamic range. A digital clock which is externally provided with 1MHz frequency from one of the rubidiums is made for recording the epoch of the fired pulse with a resolution of 1μs. We use Loran-C for epoch reference. It has been proved that the synchronization between the UTC of the Shanghai Observatory and UTC of USNO is better than 1μs by com-

parison of portable cesium clock of USNO in August 1981. We believe the time synchronization of our system with UTC of USNO is better than 3μs.

The tracking mount is still the old one, but has been slightly reformed, two new guiding telescopes with apertures of 150mm are installed.

The ranging experiments, mainly to GEOS-3, were made with the above-mentioned Nd:YAG ranging system from September 1980 to January 1981. But only a few range data were obtained because of the abnormal weather and the wobbles of the old mount which was simple and crude. Most of the data have been sent to SAO and the University of Texas at Austin for reductions. The orbit elements of GEOS-3 and GEOS-1 have been weekly provided to us from SAO by telegram since July 1980.

The method of ranging to an extended-target, a retro-reflector on the top of a water power seperated by 5.6km away from the laser, is used for calibration of the ranging system. Experiments show that the error of the pulse position measurement for single shot would be 1-1.2nsec arose from the variations of the shape of the returned signals and other factors such as the timing jitter in photomultiplier. But the variation of averages of the system calibration is quite small for different returned signals in the range of 5 to 500 photoelectrons because of adopting two constant fraction discriminators(see Fig.2, each point is an average of 20 measurements). The variation of calibration averages during a time-interval may be used to verify system stability and the experiments showed that the short-term stability of our system was about 4cm(see Figure 3). Taking all errors in account, the total range accuracy for single shot is about 20-30cm. The budget of errors of our ranging system is given in table 2. The estimation is basically supported by the preliminary analysis for GEOS-3 laser ranging data[4], and

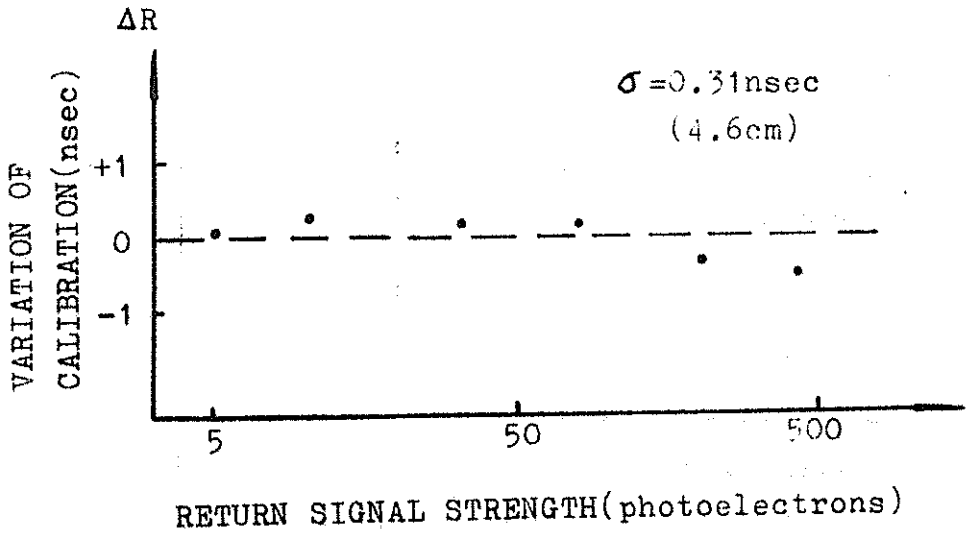

FIG.2

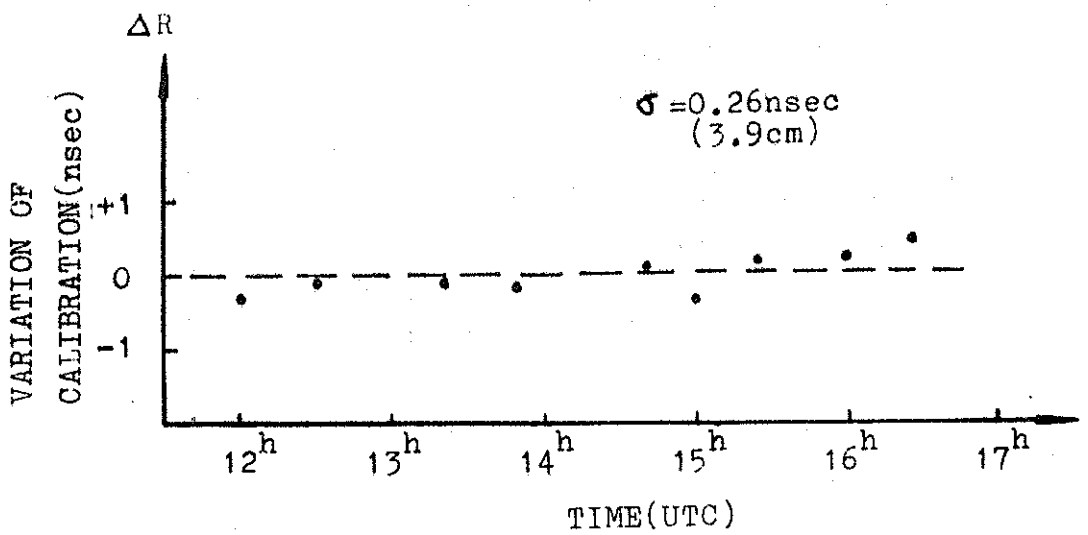

FIG.3 SHORT-TERM STABILITY OF Nd:YAG RANGING SYSTEM

Table 2 Error Budget of Nd:YAG Experimental Ranging System (4-5 nsec)

	(cm)
measuring error of counter	4.5
pulse position measurement	15-18
system stability(drift)	4
corner cube array	9
atmospheric correction	5
clock synchronization	2
total range accuracy(r.m.s.)	20-22

figure 4 shows the range residuals obtained from one pass orbit for GEOS-3 in 3 January 1981. The analysis has also shown that there is no obvious systematic error in our laser range data.

4. A Brief Description of the Second-generation Ranging System

The second-generation satellite laser ranging system has been being developed since 1978 by our observatory in collaboration with several institutes of the Academia Sinica which has long been supporting the work. The main goals of the new system are:

1. ability to track Lageos and other low orbit satellites (including Space Shuttle);
2. 10-20cm range accuracy;
3. automatic tracking with a microcomputer system.

Table 1 also lists the characteristics of the new system. Table 3 lists the main performance of the mount and servo subsystem. Fig.5 shows the optical scheme of the mount. The 600mm aperture receiver telescope is of R-C configuration, and a dichroic beamsplitter reflects almost all laser wave-

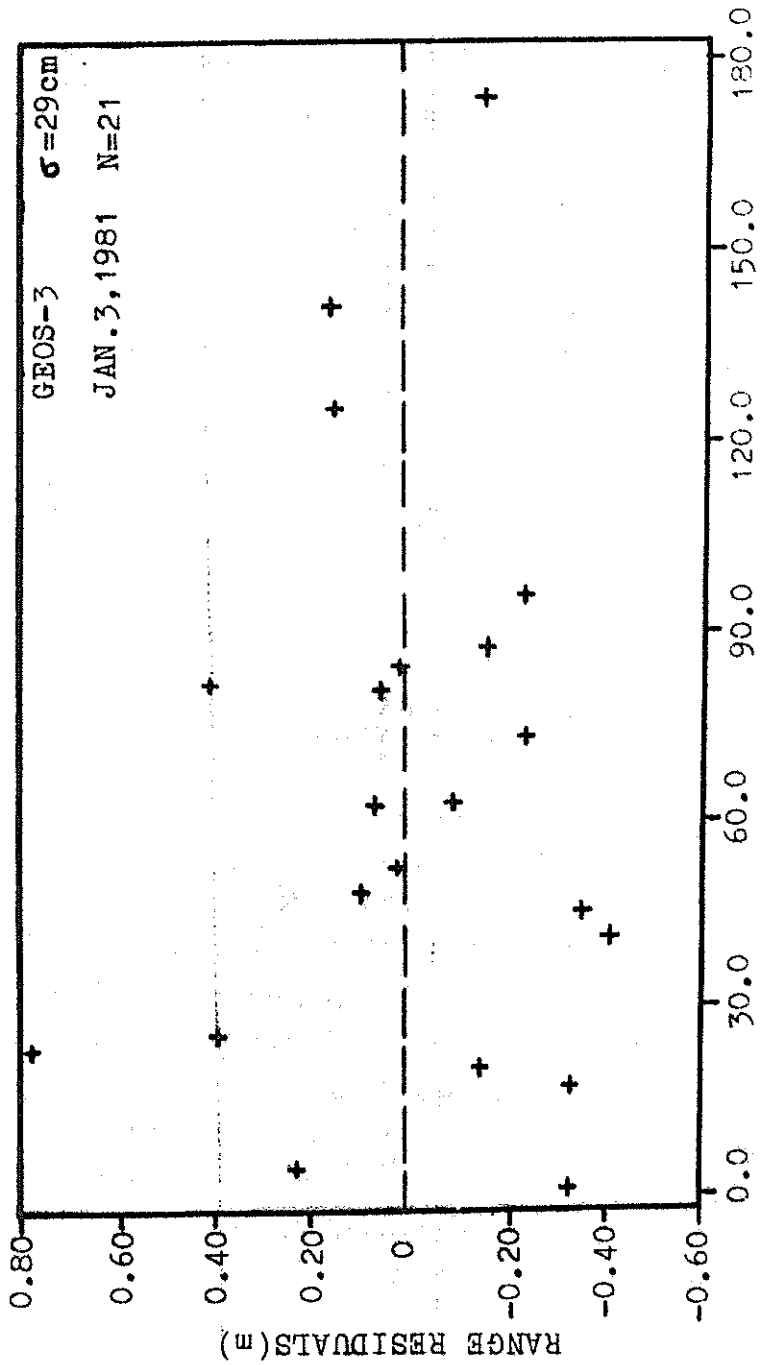

FIG.4 LASER RANGE RESIDUALS FOR GEOS-3, JAN.3, 1981

Table 3 Main Characteristics of Mount and Servo-System

Type of Mount	Altitude-azimuth and Coude optics
Range of travel	-5°—$+185^{\circ}$ in altitude
	$\pm 270^{\circ}$ in azimuth
Orthogonality	$\leqslant \pm 2$ arc second
Wobble	$\leqslant \pm 1$ arc second
Optical Encoders	20 bit, $< \pm 1.5$ arc second
Static Pointing Accuracy	+10 arc second(designed goal)
Servo System	Two axes are directly coupled torque motors, torque: 8kg-m in altitude 40kg-m in azimuth
Computer	Z-80 microcomputer system
	8 bit, 64k
	disk, printer

lenǵth(5320Å) onto photoreceiver and allows the rest wavelengthes pass to the 45° bending mirror, and then to an eyepiece for guiding faint satellites(such as Lageos), it will be effective when the automatic tracking part is out of order or when the predictions of some fast and weak satellites are occasionally inaccurate. A joystick is prepared for the visual track mode, and a 150mm aperture quiding telescope is used for tracking the low orbit satellites. Another 150mm aperture telescope is the transmitter of laser, but the 600mm primary mirror could be used for a transmitter after some modifications, if it is neccesary in future.

Now, the frequency doubled Nd:YAG laser has been completed, the receiving telescope and the mount have been being assembled and adjusted. We expect that the new system will be installed at Zô-Sè section by the fall of 1982, and will participate in the MERIT main campaign in 1983. We also intend to do the intercontinental time synchronization experiment with laser ranging technique.

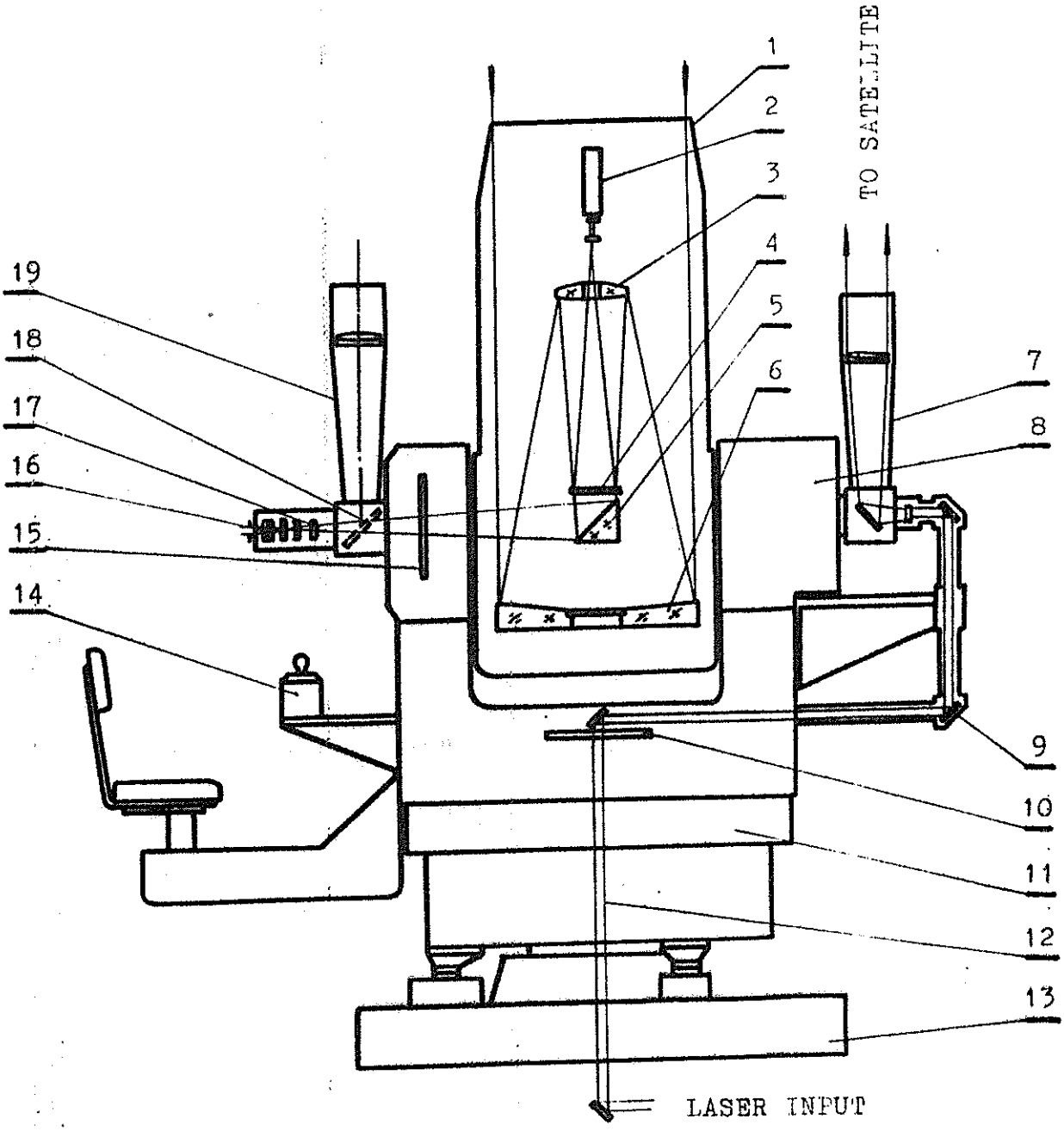

FIG.5 SCHEMATIC OF MOUNT AND OPTICS OF SECOND-GENERATION RANGING SYSTEM AT SHANGHAI OBSERVATORY(IN CONSTRUCTION)

FIG.5(continued)

1.RECEIVER TELESCOPE
2.PHOTOMULTIPLIER
3.SECONDARY MIRROR
4.DICHROIC BEAMSPLITTER
5.45° BENDING MIRROR
6.PRIMARY MIRROR(600mm)
7.TRANSMITTER TELESCOPE(150mm)
8.ALTITUDE TORQUE MOTOR AND D.C.TACHOMETER
9.45° DIELECTRIC COATED MIRROR
10.OPTICAL ENCODER(AZIMUTH)
11.TORQUE MOTOR AND D.C. TACHOMETER(AZIMUTH)
12.COUDE OPTICAL PATH
13.PIER
14.JOYSTICK
15.OPTICAL ENCODER(ALTITUDE)
16.QUIDING EYEPIECE
17.CORRECTING LENS
18.45° FLIP MIRROR
19. QUIDING TELESCOPE(150mm)

We are gratefully indebted to Prof.Ye Shuhua and Prof. Wan Lai for their supports and encouragements in this work.

This laser ranging group consists of Yang Fumin, Zhu Youming, Shi Xiaoliang, Tan Detong, Lin Qinchang, Zhang Yanlin, Su Jinyuan, Liu Jiaqian and other colleaques. This paper is presented by Mr.Cheng Hao, one of the members of our group, who has stayed at the University of Texas at Austin for a short-term work.

References

1. Yang Fumin, et al., The Satellite Laser Ranging System at Shanghai Observatory, Annals of Shanghai Observatory, No.1, 83, (1979).
2. Lin Qinchang, Niu Xiulan, A Method for Acquiring the Tracks of Artificial Satellites, Ibid,, 92, (1979).
3. Yang Fumin, et al., A Satellite Laser Ranging System with Decimeter Precision, Science Bulletin, (1981), (in English, in press).
4. He Miaofu, et al., A Preliminary Estimation of Accuracy for GEOS-3 Laser Range Data from Shanghai Observatory, (1981), to be published.

Table 1 Performances of the Satellite Ranging Systems at Shanghai Observatory

	first generation system	Nd:YAG experiment. system	second generation system
Laser subsystem			
material	ruby	Nd:YAG	Nd:YAG
output wavelength	6943Å	5320Å	5320Å
type	single oscillator	oscillator, amplifier, freq. doubl.	oscillator, two amplifiers freq. doubler
output energy	2.5j	80-100mj	250mj
width of pulse (FWHM)	25ns	4-5ns	4-5ns
repetition	0.5pps	0.5pps	1pps
Q-switch mode	dye-cell	$LiNbO_3$ crystal	$LiNbO_3$ crystal
Transmitting Optics			
type	galilean	galilean	galilean and coudé optics
aperture	120mm	42mm	150mm
beam divergence	1 mrad	0.3-0.8mr	0.2-2 mrad
Receiver			
aperture	300mm	300mm	600mm
field stop	3 mrad	2 mrad	0.2-2 mrad
filter bandwidth	60 Å	27 Å	5-7 Å
type of PMT	EMI9558	GDB-49	GDB-49, RCA C31034A
quantum effeciency	3%	10%	10-24%
risetime	10ns	2ns	2ns
gain	5×10^6	3×10^7	10^6-3×10^7
resolution of timer	10ns	0.1ns	0.1ns
Quiding Optics			
type	sighting scope	sighting scope	receiver telescope with a dichroic beam-splitter, sighting scope
aperture	90mm	150mm	600mm; 150mm

(Table continues)

Table 1 (Continued)

field of view	4°	3°	30'; 3°
Type of Mount	alt-az	alt-az	alt-az and coudé optics
Time System			
freqency standard	quartz oscillator	rubidium (2 sets)	rubidium (2 sets)
stability	1×10^{-8}/day	3×10^{-12}/day	3×10^{-12}/day
synchronization	microwave	Loran-C	Loran-C
accuracy of synchr.	50 μs	3 μs	3 μs
General			
range accuracy	1-2 m	20-30cm	10-20cm
maximum range	2700km	2000km	over 7000km
tracking mode	visual	visual	microcomputer control, and joystick
Time in Operation	1975	1980	in construction (1982)

Satellite laser tracking. Construction of normal points

D. GAMBIS

GRGS/BIH

Abstract

Many stations, in particular in the NASA network, have an observational rate of about one measurement per second. For a 45 mn pass of Lageos, this gives more than 2000 measurements. Processing the whole data set is a heavy task, so a sampling of data is performed to reduce the number of points to 100 or 200 over a satellite pass. This solution, currently used is not satisfactory for it leads to a loss of information. Data compression, taking into account the full rate measurements has been carried out to give about 10 to 15 normal points over a pass. The method uses the approximation by the Tchebycheff polynomial expansion. The devised software can be easily implemented with mini-computers, so that every tracking station taking part in a worldwide network would be able to calculate from its own data, normal points to be forwarded to a computing center for the global processing. Data compression permits also to reduce the local random noise of an order of magnitude. The method has been applied to a limited data interval of Merit campaign.

I Introduction

Let D(t) be the discrete function representing the distance station-satellite during a pass. This distance varies approximatively

from 6000 to 10 000 km for a Lageos arc and the duration of the tracking is about 45 mn. Depending on the capability of the station, observation densities are around 1 per second for NASA stations, some units per mn for other ones. Of course, laser observations require clear weather and all passes don't offer good data distribution.

The idea of making normal points consists in compressing the information contained in a certain number of measurements into one data. To make this compression, one has to find a good representation of the function D(t). Two main philosophies are possible ;

a) Using a model of forces, a good reference orbit is computed for several revolutions of the satellite. Pseudo-measurements are calculated from the difference between the arc of the reference orbit and the corrected arc (Lago and Mainguy 1971). The main drawback of this method is its heavyness ; it requires elaborate orbit computation with several data files for the models of forces introduced.

b) The function D(t) may be approximated by analytical expressions, for instance polynomial expansion. It is what we have chosen in this study.

II Simulation.

In order to investigate the faisability of the method, simulations have been made. A 45 mn orbit was computed using a complete model of forces and at the same time, the distances station-satellite, representing the measurements, have been generated at 1 second intervals. The simulated pass is considered as perfect without uncertainties on the data. The normal points must be restituted with an inaccuracy, say, an order of magnitude inferior to the nominal accuracy of the laser tracking station (i.e. about 1 cm). We have tried to approximate the function D(t) over a pass, through different representations ;

1) Low-order polynomial representation.

We did not intend to restitute directly D(t) with the 1 cm precision but, in a first step, to remove of it most of the variations. A fourth order polynomial $P_4(t)$ was found to best fit the observations. $[E_4(t) = D(t) - P_4(t)]$. Residuals $E_4(t)$ are between - 6 km and + 3 km.

A Vondrak smoothing (Vondrak 1977) is then performed onto

$E_4(t)$. The optimal smoothing will be the strongest one restituting the 1 cm precision.

We have $E'_4(t) = E_4(t) - V(t,\varepsilon)$

represents the smoothing strength

$$\varepsilon = 10^{-n} \quad n \in N$$

For $\varepsilon = 1$ the smoothing fits all the points, for $\varepsilon = 0$ it is a parabole. The analysis of the perturbations of the satellite-trajectory due to the earth gravity field shows no effect of wavelength inferior to 45 mn.

We can see from figure 1 than values of $\varepsilon = 10^{-n}$ may be tested for $n \geq 6$.

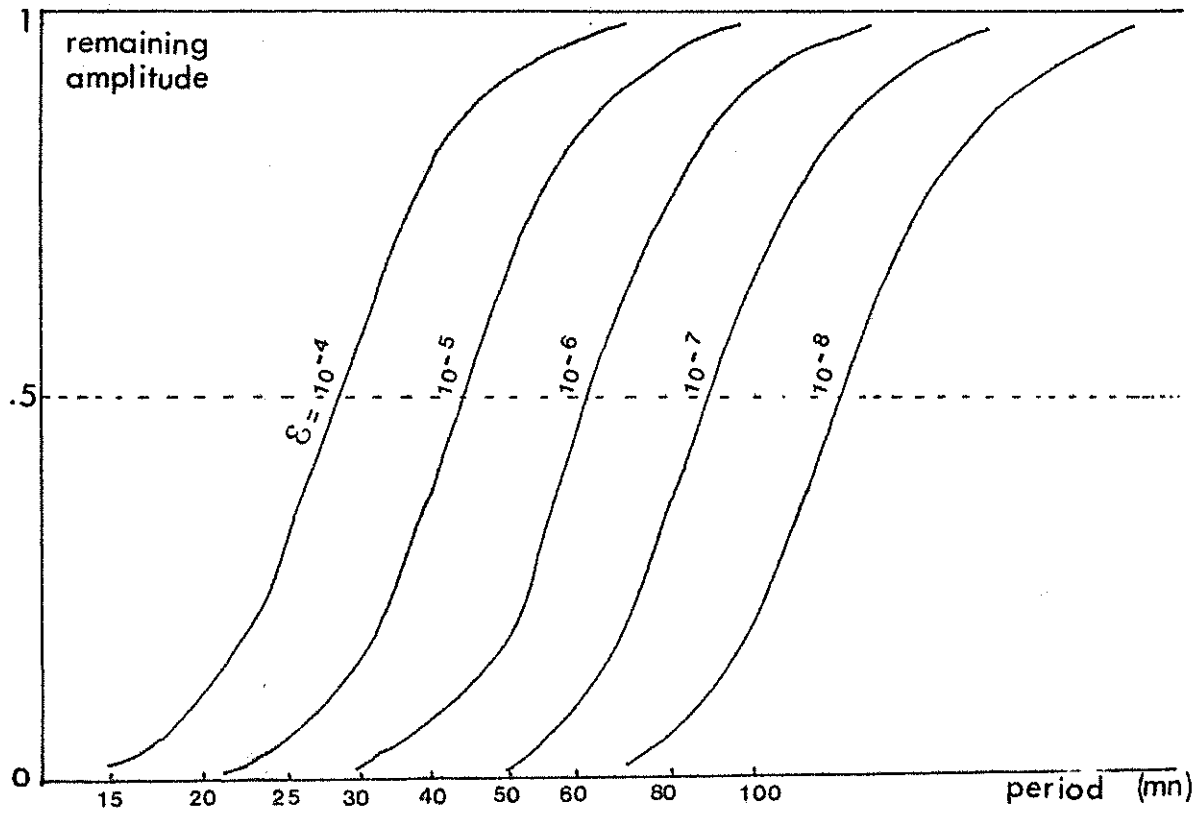

Figure 1. Filter corresponding to different degrees of smoothing (characterized by ε)by Vondrak's algorithm.

Table 1 shows the values of the root-mean square of the residuals $E'_4(t)$ with respect to the smoothing.

Smoothing coefficient	root-mean square of $E'_4(t)$ with respect to the smoothing (in cm)
10^{-6}	12.4
10^{-7}	47.0
10^{-8}	172.3

Table 1. Simulated pass-smoothing of the residuals to a 4th order polynomial fit.

The inadequacy of the polynomial fit, particularly at the extremities of the interval (Gibbs phenomenon), is in fact responsible of the impossibility of reaching the 1 cm precision. This leads to the idea to use a more sophisticated parametrized representation using polynomial expansions.

2) Tchebycheff polynomial expansions have been used for several years by the Bureau des Longitudes for ephemeris calculations (Connaissance des Temps). Among other polynomial expansions (Hermite, Laguerre, Lagrange, Legendre) Tchebycheff's ones have simple expressions.

Their form is

$$P_n(t) = \sum_{k=1}^{n} C_k \; T_k(t)$$

n order of the expansion

$T_k(t)$ Tchebycheff polynomial of k^{ieth} order

$T_k(t) = \cos(k \arccos t)$

C_k are defined as

$$C_o = \frac{1}{n} \sum_{i=0}^{n-1} P_n(t_i)$$

$$C_k = \frac{2}{n} \sum_{i=0}^{n-1} P_n(t_i) \cos \frac{k\Pi}{2n} (2i + 1)$$

$$\text{with } t_i = \cos \frac{\Pi}{2n} (2i + 1)$$

Further details can be found in mathematical handbooks (as J. Legras 1963). We have used the software of interpolation and approximation by Tchebycheff polynomial expansions implemented by J. F. Lestrade (1976) for a study about the representation of the attitude of the astrometric satellite Hipparcos.

Over the pass interval I

$$E_n(t) = D(t) - P_n(t)$$

is the error of the representation of D(t) by $P_n(t)$. The size of this error can be characterized by a norm

$$M_n = \sup_{t \in I} |E_n(t)| \qquad \text{maximum error}$$

$$\text{or} \quad s = \sum_{t \in I} E_n(t)^2 \qquad \text{quadratic error}$$

The "best approximation" of D(t) on I can be defined as the polynomial expansion yielding either M_n or s minimal.

Application to a simulated pass.

The table 2 gives, function of the expansion order, the values of the two norms

expansion order	$M_n = \sup_I \lvert E_n(t) \rvert$ (in cm)	$s = \sum_I E_n(t)$ (in cm)
12	270.0	148.0
14	29.0	15.0
16	4.3	1.7
18	2.1	.6
20	1.3	.5
22	.8	.5
24	.6	.4
26	.6	.4

Table 2. Simulated pass. Convergence of the residuals to a Tchebycheff representation.

The requirement of the 1 cm precision is fulfilled ; the method can be applied to real data.

III Case of real data.

1) Example of application to dense passes.

A first approximation is performed with an expansion order n = 8 ; the procedure is iterated (n = n + 2) until the determination of the "best approximation" (with respect to the quadratic norm s).

When the root-mean square between two consecutive values is stable (i. e. the difference is inferior to a preset quantity) the convergence is declared. During this procedure, identification and deletion of spurious data is done on the basis of the comparison of their residuals to the global root-mean square.

For construction of normal points the pass is cut into 3 mn intervals I_P. The datation of the normal point t_p is chosen to be the closest possible to the center of the interval (at a real data datation), in order to avoid new interpolation and for use of the calculated refraction correction usually transmitted with the observational data.

The value of the normal point is

$$N(t_P) = P_n(t_P) + \frac{1}{n_P} \sum_{j=1}^{n_P} E_n(t_j)$$

this for dense passes when the residuals $E_n(t_j)$ are gaussian. A typical histogram of the number of the residuals with respect to their values is shown figure 2, the mean of the residuals is different of zero.

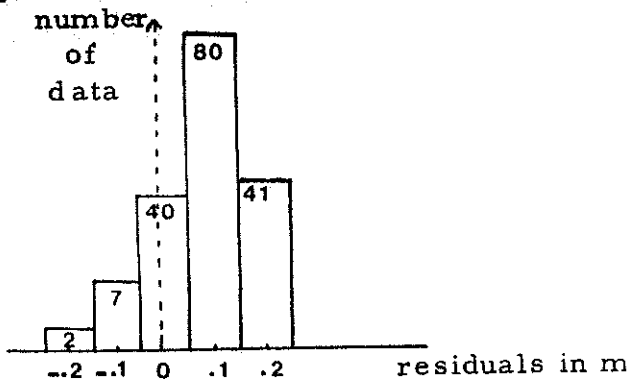

Figure 2. Dense pass histogram number of data per residual interval for station Yarragadee (7090).

Figure 3 represents the residuals (raw data -Tchebycheff representation) over a pass of station Grasse (7835). For most of the 3 mn normal intervals, the residual function is gaussian.

For other passes with small density of observations (some per mn) the residual function is usually not gaussian over the 3 mn intervals (fig. 4). The averaging should be made by another way.

In case where $E_n(t)$ is gaussian over the 3 mn interval I_P, the root mean square of a single residual with respect to the mean $\frac{1}{n_P}\sum E_n(t)$ is :

$$\sigma_{o,\,P} = \sqrt{\frac{n_P \sum E_n(t)^2 - \left(\sum_{I_P} E_n(t)\right)^2}{n_P\,(n_P - 1)}}$$

To take into account the number of data n_P in I_P the root-mean square of the normal point will be

$$\sigma_P = \sigma_{o,P} \sqrt{\frac{1}{n_P}}$$

When the number of data is small ($\lesssim 5$) over I_P the expression herebefore of σ_P has few signification. In this case, a conventional expression has to be chosen for σ_P, for example

$$\sigma_P = \sigma_o \sqrt{\frac{1}{n_P}}$$

σ_o being the root-mean square of the whole pass with respect to the fitted representation.

To avoid an overweight of the normal points of some stations compared to the others it will be necessary to give an inferior limit to their σ_P.

Tables 3 to 5 show the observational normal points of typical passes of different laser tracking stations : Yarragadee (7090), Haystrack (7091), Grasse (7835), Orroral (7943) and Arequipa (7907).

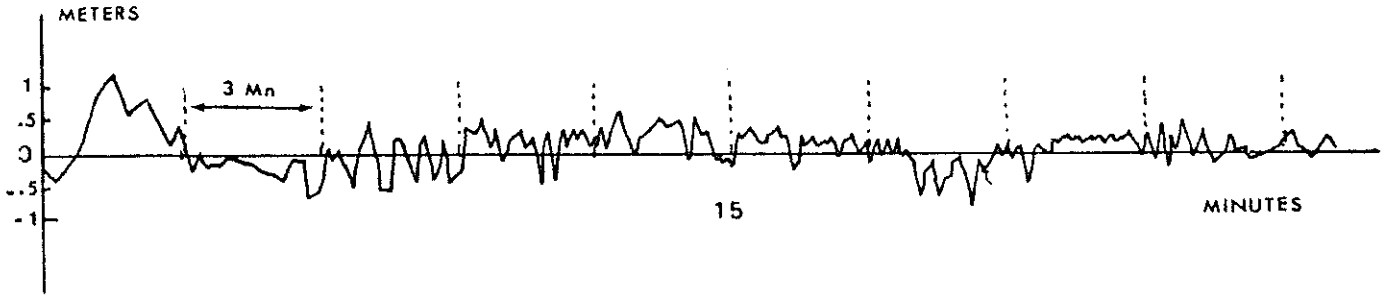

FIGURE 3 GRASSE (7835). Residuals over a dense pass

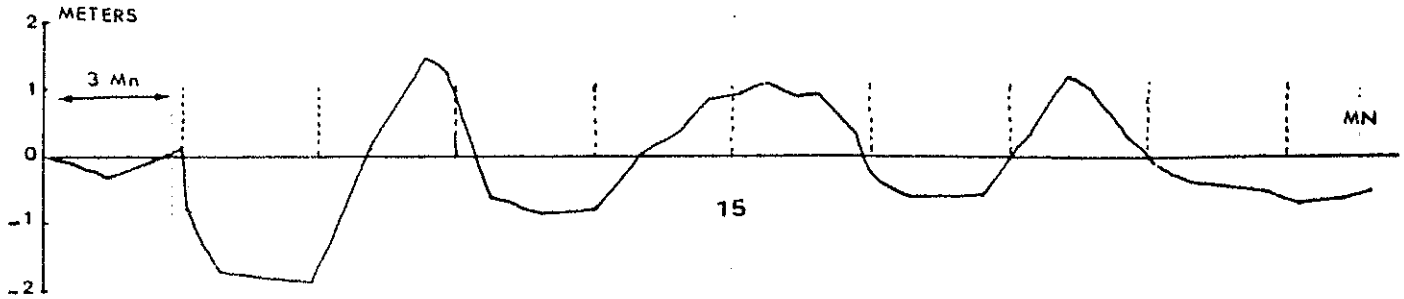

FIGURE 4 GRASSE. Case of a pass with a poor data distribution

NORMAL POINTS EVERY 180. S STATION 7090 DAY = 219 PASS 18 H 2 MN

LENGTH OF THE PASS = 31. MN NUMBER OF DATA = 1514 DENSITY =48.7 MES. PER MN

DATE IN SECONDS	NORMAL POINT(M)	SIGMA(M)	NUMBER OF DATA
65055.024823	7291576.196	.008	135
65235.023828	6993460.851	.008	140
65414.023085	6770529.905	.008	151
65594.022617	6630111.008	.007	154
65773.022451	6580632.286	.010	127
65954.022599	6624847.583	.009	151
66134.023063	6760928.643	.008	170
66314.023793	6982690.143	.009	132
66494.024787	7280812.034	.006	170
66673.025992	7642081.960	.009	120
66827.027173	7995987.556	.017	39

NORMAL POINTS EVERY 180. S STATION 7091 DAY = 214 PASS 9 H 13 MN

LENGTH OF THE PASS = 46. MN NUMBER OF DATA = 2096 DENSITY =45.4 MES. PER MN

DATE IN SECONDS	NORMAL POINT(M)	SIGMA(M)	NUMBER OF DATA
33329.033575	8102650.880	.110	31
33509.032098	7659847.325	.025	74
33689.030749	7255330.624	.016	124
33868.029569	6901499.131	.012	155
34048.028582	6605700.550	.011	169
34228.027834	6381398.543	.010	176
34408.027358	6238692.904	.008	176
34588.027179	6184952.424	.006	173
34768.027307	6223487.879	.008	168
34948.027739	6352903.572	.011	172
35128.028455	6567416.254	.010	175
35308.029424	6857988.652	.009	171
35488.030611	7213804.507	.012	143
35655.031873	7592435.559	.027	25
35849.033497	8079238.527	.025	73
35998.034834	8480065.516	.042	17

Table 3. Observational normal points for YARRAGADEE (7090) and HAYSTACK (7091).

NORMAL POINTS EVERY 180. S STATION 7835 DAY = 268 PASS 20 H 33 MN

LENGTH OF THE PASS = 34. MN NUMBER OF DATA = 213 DENSITY = 6.2 MES. PER MN

DATE IN SECONDS	NORMAL POINT(M)	SIGMA(M)	NUMBER OF DATA
74178.419422	7667431.525	.187	8
74308.418851	7385276.923	.073	15
74493.419633	7038015.392	.081	20
74658.405520	6791393.727	.065	22
74843.384960	6596337.070	.051	26
75028.382256	6496275.659	.034	28
75203.374117	6493737.522	.064	21
75388.371423	6588390.756	.041	28
75568.433195	6771716.180	.053	15
75743.465609	7027917.738	.041	18
75923.343449	7360653.731	.040	9
76078.416694	7695067.734	.219	2

NORMAL POINTS EVERY 180. S STATION 7835 DAY = 323 PASS 19 H 31 MN

LENGTH OF THE PASS = 40. MN NUMBER OF DATA = 215 DENSITY = 5.4 MES. PER MN

DATE IN SECONDS	NORMAL POINT(M)	SIGMA(M)	NUMBER OF DATA
70379.151165	8433620.657	.143	14
70574.139353	8001245.100	.093	15
70754.116162	7656231.990	.103	20
70934.167699	7373625.228	.060	16
71114.188048	7163397.833	.072	18
71299.150107	7031309.871	.083	9
71474.162679	6989902.833	.075	23
71659.155714	7036306.990	.108	21
71834.132708	7163365.241	.091	18
72014.179387	7372834.768	.108	18
72184.195106	7636452.918	.112	11
72374.200836	7996267.958	.108	13
72554.191649	8389932.663	.185	15
72699.178368	8737395.459	.353	2

Table 4. Observational normal points for GRASSE (7835).

NORMAL POINTS EVERY 180. S STATION 7943 DAY = 218 PASS 19 H 17 MN

LENGTH OF THE PASS = 12. MN NUMBER OF DATA = 79 DENSITY = 6.3 MES. PER MN

DATE IN SECONDS	NORMAL POINT(M)	SIGMA(M)	NUMBER OF DATA
69547.550798	7756274.611	.079	10
69727.480796	7460786.461	.071	20
69907.450796	7225638.910	.089	22
70087.450797	7058088.086	.046	23
70199.930796	6990246.336	.191	3

NORMAL POINTS EVERY 180. S STATION 7907 DAY = 217 PASS 9 H 17 MN

LENGTH OF THE PASS = 38. MN NUMBER OF DATA = 135 DENSITY = 3.5 MES. PER MN

DATE IN SECONDS	NORMAL POINT(M)	SIGMA(M)	NUMBER OF DATA
33570.030776	7193551.064	.215	7
33750.040777	6817125.741	.215	7
33930.160777	6506930.794	.129	10
34102.660777	6283498.590	.166	15
34267.560777	6146025.484	.145	12
34462.560777	6087256.934	.175	15
34650.080777	6139556.805	.163	16
34837.580777	6294986.591	.204	8
35010.080777	6521321.762	.181	11
35175.080777	6803254.297	.150	8
35355.080777	7172289.317	.215	7
35542.580768	7611795.641	.179	8
35707.580775	8034772.430	.254	5

Table 5. Observational normal points for ORRORAL (7943) and AREQUIPA (7907).

2) Example of a complete processing

The procedure for the construction of normal points has been applied to a 5 day data span of august 1980 (Merit Campaign) for NASA and SAO tracking stations.

For dense passes (several tens per minute) with good data distribution, the "best approximation" is easily reached with about 20 Tchebycheff coefficients. In some cases, however, the identification of bad data is not correctly done ; the procedure has to be refined.

For passes with weak number of data or with low observational rate (some measurements per minute) the procedure, because of the interpolation method, does not seem to be adapted.

A preliminary orbit computation with the pole components determination, has been performed over a 5 day interval. Although many passes have been deleted in the normal points constructions, the results obtained are equivalent to these obtained during the same period using a sampling of the data. The values of the computed pole components are given table 6.

	Pole computation with sampling of data	Pole computation with normal points	BIH Circ. D
Number of data	2308	195	
x	- .009	- .057	- .024
σ_x	.008	.020	
y	.317	.306	.304
σ_y	.004	.009	

Table 6. Pole components determinations using the sampling of data and the normal points.

IV Conclusion. Advantages, limitations and possibilities of the method.

Tchebycheff polynomial expansions seem well adapted for the construction of normal points when measurements are dense enough during a pass.

The software may be easily implemented on mini-computers. The algorithms have to be refined to take into account the multiplicity of the data distributions ; yet for passes with low density data, another treatment has to be used.

The root-mean square associated with normal points is optimistic. The normal points values, depending on the polynomial representation are correlated. To minimize the dependence, good methods for averaging the residuals (raw data - representation) are required.

Within the framework of the organization of an earth rotation service, each laser tracking station using this procedure or a similar one, could reduce its own data in order to send normal points to this service. The volume of data may be highly reduced (see the annex). The task of the processing to calculate the earth rotation parameters would be lightened and the delay of availability of the results shortened.

References.

B. Lago and A. M. Mainguy. Condensation des données d'observation en vue d'une utilisation géodésique. Space Research XI. Akademie Verlag, Berlin 1971, p. 515.

J. Legras. Précis d'Analyse Numérique. Ed. Dunod 1963.

J. F. Lestrade. Communication personnelle.

J. Vondrak. Problem of smoothing observational data. Bull. Astron. Inst. Czech. 28 (1977), p. 84-89.

A N N E X

	Number of characters
Satellite	6
Station	4
Meteorological data	10
Date (year, day)	6
Center of mass correction	4
Various indexes	4
Total	34

General informations over the pass

	Number of characters
Datation (μs)	11
Measurement normal point(mm)	11
Sigma (mm)	5
Tropospheric correction (mm)	5
Total per normal point	32

Information per normal point

for the whole pass (14 normal points) 34 + 32 x 14 = 482 characters

So about 3/1000 of the global volume transmitted in format SEASAT

Number of characters sufficient for representing a pass. Example of a 40 mn pass with 2000 data.

AN EVALUATION AND UPGRADING OF THE SAO PREDICTION TECHNIQUE

J. H. LATIMER, D. M. HILLS, S. D. VRTILEK,
A. CHAIKEN, D. A. ARNOLD and M. R. PEARLMAN

ABSTRACT

We review the current SAO prediction system capability and discuss recent improvements that show results for 60-day test prediction periods for Lageos. The improvement package is machine-accessible.

OVERVIEW OF THE CURRENT SYSTEM

The current prediction system at SAO is based upon two key programs: an orbit determination program (GRIPE) used at the central computation facility in Cambridge, and a look-angle and predicted range generator program used at field sites (FLPPS). Observations obtained at field sites are fed to the GRIPE program, and Keplerian elements derived from GRIPE are supplied to the FLPPS program. This data flow is the basis of the tracking cycle.

GRIPE is a general purpose orbit analysis program for artificial earth satellites which has been developed as a research tool. It is based primarily on analytical perturbation theory and can take as observations a variety of data types including optical or electronic direction observations, ranging data, range rate or velocity data, and altimetric ranging data. In addition to computing orbital elements, GRIPE can solve for corrections to the gravity field coefficients, station coordinates, frequency offsets and drift rates for range rate observations, the earth's

pole position, the gravitational constant GM, and an earth radius scale factor.

GRIPE is a differential improvement program requiring that initial estimates for modelling parameters be reasonable in order that convergence of iterated solutions can occur. The observation model computes the vector between the observing site and the satellite and must consider perturbations to both positions. Perturbation theory applied to the satellite position includes the following:

1. Kinoshita's Short Periodic Oblateness (to first and second orders in J2, and optionally to third order),
2. Gaposchkin's Tesseral Harmonics development,
3. Kozai's Direct Lunar and Solar effects (both long and short periodic),
4. Kozai's Body Tide treatment (due to both Lunar and Solar effects),
5. Kinoshita's Long Periodic Zonal Harmonics to first and second orders. Other perturbations not used in acquisition ephemeris work are:
6. Doodson's Ocean Tide effects (lunar and solar),
7. Kinoshita's reference system adjustment,
8. Aksnes' Direct Effect Radiation Pressure,
9. Lautman's Albedo and Infra-red effects.

Station positions are adjusted for the effects of UT1 (when known), for pole position, and for the effect of solid earth body tides due to the sun and moon.

The observed quantity relating the station and the satellite is reduced for the tropospheric or parallactic refraction, and if ranging data, for the offset between the center of mass and the reflector array and a small general relativity effect.

GRIPE has the capability of displaying the observation residuals and then halting execution before improving any modelling parameters. This mode of operation is known as a "residual run", and is a basic tool used in the analysis of prediction orbit quality described below.

UPDATING

The motivation for upgrading prediction accuracy at SAO is to be able to tighten the range gate for better discrimination against noise pulses in the return pulse detection process. The improvement sought involves a mixture of software changes and procedural changes. Changes to the GRIPE orbit determination are purely procedural in that no coding changes are necessary. Our testing shows that we would benefit by lengthening the data span for orbit determination and by holding constant some orbital parameters more accurately determined over long term studies. These parameters include the rate of perigee, and the quadratic term in mean anomaly. Our tests have no rate of eccentricity or inclination in the model, which differs from our current operational technique. The final change in the GRIPE procedure is the inclusion of solar perturbations, both long and short periodic. The current technique absorbs to a certain extent these effects in the mean elements.

For the field program, FLPPS, the changes are algorithmic, in that the older analytic lunar perturbation package, which only computed the principal lunar term, has been replaced with a lunar perturbation package identical to that in GRIPE. This package is a numerical integration package and facilitates now the computation of the solar perturbations as well, so that the FLPPS has this additional capability.

Users of the SAO orbital element service would do well to consider including this a)improved lunar and b)solar perturbation capabilities for the following reasons:

1. Obtaining improved prediction accuracies as demonstrated below.
2. Avoiding the problem of incompatibility between field software expecting solar perturbations to be absorbed into the determination of mean elements (the present situation) and orbit computation expecting solar perturbations to be separately and explicitly applied.
3. The key routines are available separately in machine-accessible form in order to ease the task of updating code.

RESULTS

As it is impractical to try prediction experiments with an operational network, our measurement of prediction quality decomposes into two stages. The first stage is to demonstrate that the central facility and the field site software are in agreement in terms of orbit theory as manifested by the computation of angles and ranges between stations and satellites. This stage does not address the issue of inherent quality of representation of a trajectory, but only that of consistent algorithmic treatment of an orbit model. This may be done with simulations or other analytic methods. Our tests (see figure 1.) indicate that this agreement is within the noise of the method of testing for about 30 days and within 0.25 microsec of range gate for about 60 days using the LAGEOS orbit. This is the software implementation, or "ZEROSET" test.

The other aspect is that of the quality of an orbit as a description of a satellite trajectory, and this can only be measured with real observational data, and thus we are obliged to use data archives to draw conclusions. However, having done the ZEROSET test, we are here unconcerned with software compatibility and can test the orbit extrapolation qualities with the orbit determination program run in residual mode. Figure 2 shows the extrapolation over time of an orbit of LAGEOS obtained with the current operational procedure. Next, we see a factor of two improvement when the solar perturbation is added. Some additional improvement is noticeable when the test orbit is generated with data from seven stations instead of only one station. Further improvement is noticed when the test orbit is generated from 18 instead of 9 days of data. When the rate of perigee and the quadratic term in mean motion are fixed still further improvement is noticed although there is no significant difference in the orbits obtained from 18 and 9 days of data. These last orbits, as the figure shows, are within 0.50 microsec of range gate for about 30 days.

These tests were performed with data from the summer of 1981, and to confirm these results the final test (18 days, fixed rate of perigee and quadratic term in mean motion) was performed with data from the fall of 1980. The results of this test are shown in figure 3. These results are similar to the above, which suggest that even better results could be obtained by using rates obtained from long-term analysis. Further study ought to also consider any effects from degradation of elements other than mean anomaly, which is emphasized in this analysis.

ACKNOWLEDGMENT

This work was supported by Grand NGR 09-015-002 from the National Aeronautical and Space Administration.

REFERENCES

Brown, E. W., 1908, "Theory of the motion of the Moon; containing a new calculation of the expression for the coordinates of the moon in terms of the time." Mem. Royal Astr. Society 53.

Cartwright, D. E., and A. C. Edden, 1973, Corrected table of Tidal Harmonics" Geophys. J. 33:253-264.

Doodson, A. E., 1921, The harmonic development of the tide-generating potential. Proc. Roy. soc. A. 100: 305-329.

Gaposchkin, E. M., 1970, "Improved values for the tesseral harmonics of the Geopotential and Station Coordinates." Dynamics of Satellites 1969, ed. by B. Morando, Springer-Verlag, Berlin, 109-118.

Gaposchkin, E. M., 1973, Standard Earth iii, Smithsonian Astrophysical Observatory Special Report 315.

Gaposchkin, E. M. and E. Lambeck, 1969 Standard Earth III, Smithsonian Astrophysical Observatory Special Report 315.

Gaposchkin, E. M. and E. Lambeck, 1971, "The Earth's gravity field to sixteenth degree and station coordinates from satellite and terrestrial data." Journ. Geophys. res., vol. 76, 4855-4883.

Hori, G., 1973, "Theory of General Perturbations" In Recent Advances in Dynamical Astronomy, ed. by B. D. Tapley and V. Szebehely, D. Reidel Publ. Co., Dordrecht-Holland, 231-249.

Izsak, I. G., 1964, "Tesseral Harmonics of the Geopotential and Corrections to Station Coordinates." Journ. Geophys. Res., vol. 69, 2621-2630.

Kaula, W. M., 1967, "Theory of Statistical Analysis of Data Distributed over a Sphere" Rev. Geophys., vol. 5, 38-107.

Kinoshita, H., 1977, "Third-order Solution of an Artificial Satellite Theory" Smithsonian Astrophysical observatory Special Report 379.

Kozai, Y., 1973, "A New Method to Compute Perturbations in Satellite Motions" Smithsonian Astrophysical Observatory special Report 349. Modifications by Kozai were made in 1979 and 1980.

Love, A. E. H., 1908, "Note of the Representation of the Earth's Surface by Means of Spherical Harmonics of the First Three Degrees." Proc. Roy. Soc. A. 80: 553-556.

Veis, G., 1963, "Precise Aspects of Terrestrial and Celestial Reference Frames" Smithsonian Astrophysical Observatory Special Report 123.

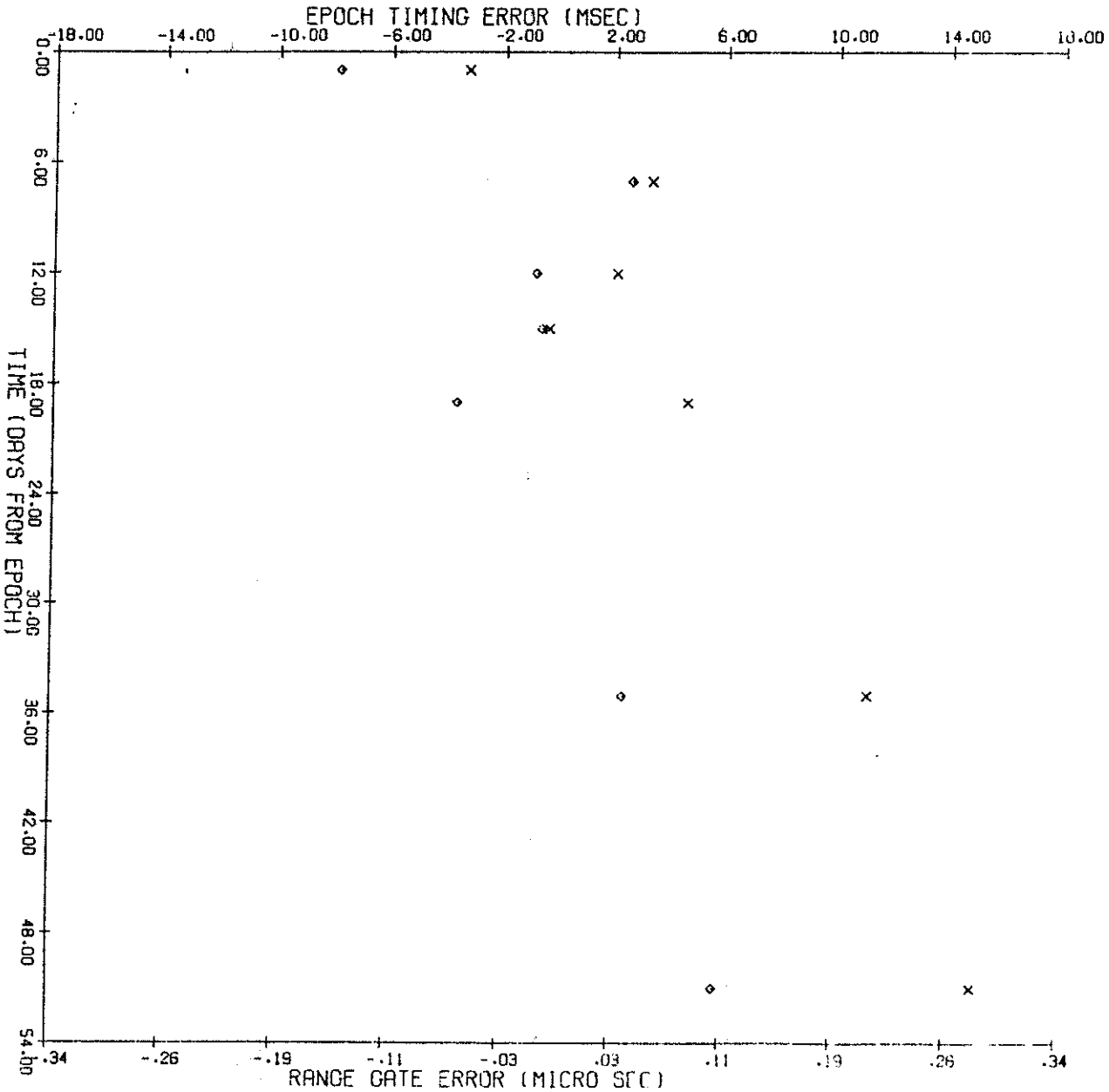

Figure 1.
"Zeroset"
Consistency between field and central software implementations (Zeroset).
New FLPPS pseudo-obs. vs. new GRIPE in FLPPS mode
X = beg.; ◊ = end obs. in each pass (≳ 30° elevation angle)

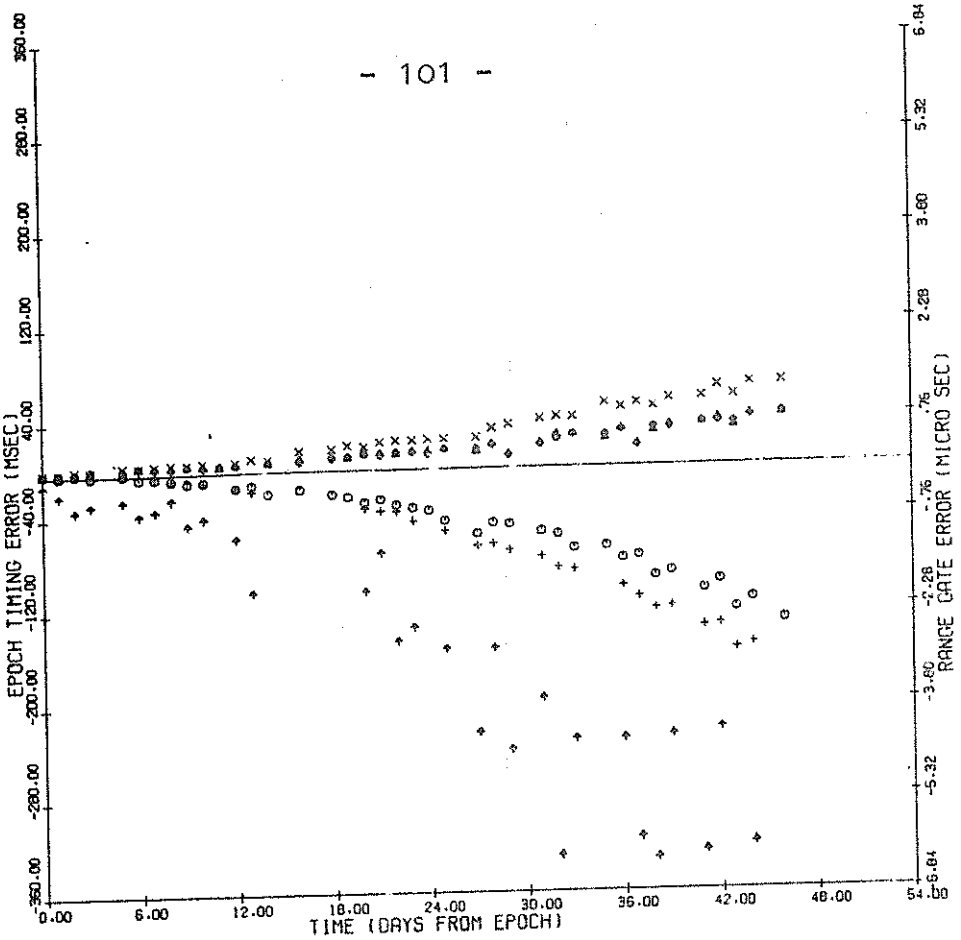

Actual data vs.:

⧫ = old GRIPE (no solar) ṅ = .5E-8	X = new GRIPE (solar) 7 station orbit (18 days) ṅ = -.5E-9
+ = new GRIPE (solar) 1 station orbit (9 days) ṅ = .7E-8	⧋ = new GRIPE (solar) 7 station orbit (9 days) fixed rates ṅ = .43E-9
⧫ = new GRIPE (solar) 7 station orbit (9 days) ṅ = .5E-8	◇ = new GRIPE (solar) 7 station orbit (18 days) fixed rates ṅ = .43E-9

Figure 2. Results of orbit quality tests. From bottom to top, series are:
a) current technique (no solar perturbation)
b) add solar, one station, 9 day arc
c) solar, 7 stations, 9 day arc
d) solar, 7 stations, 9 day arc, fix rates
e) solar, 7 stations, 18 day arc, fix rates
f) solar, 7 stations, 18 day arc

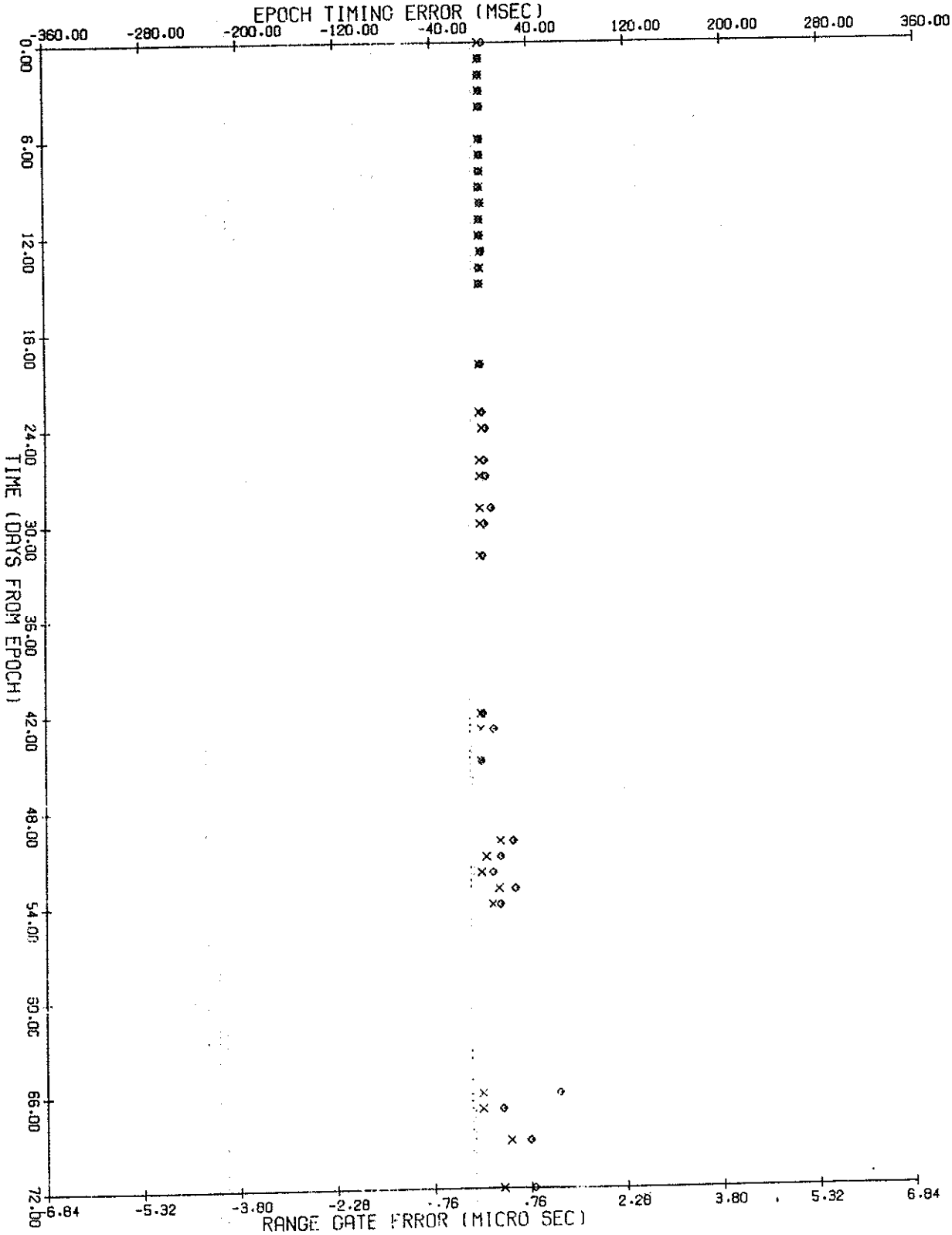

Figure 3.

Results of orbit quality tests for fall, 1980 period. Same technique as Figure 2e. In some cases, two estimates are available, X represents either second estimate or zero.

APPENDICES
LUNAR PERTURBATION OVERLAY

S. Vrtilek
May 1981

The lunar perturbation overlay uses the luni-solar perturbation theory developed by Y. Kozai as reported in Smithsonian Special Report 349. All source codes necessary for this overlay are on FLPPS Disk One.

THE SUBROUTINES USED IN THIS OVERLAY ARE:

RDZON--Loads registers with Zonal harmonics
INST--Calculates instantaneous elements at epoch of observation
GETSMA--Calculates Semi-major Axis
NFINC--Calculates Inclination function
HANSEN--Calculates Eccentricity function
FACCAL--Computes factorials
LUNARK--Calculates long period and short-period luni-solar perturbations
SETUP--Assigns variables for integration
KIND--Integrates terms for lunar and solar perturbations
SUNVECT--Calculates vector to Sun
LUNVECT--Calculates vector to Moon
PRECESS--Calculates terms due to precession
EVA--Computes sin and cos terms for eccentricity and mean anomaly

THE FUNCTIONS USED IN THIS OVERLAY ARE:

CONSOC--Stores the constants used in overlay
ERIQA--Solves Kepler's equation
LOAD--Takes lower order 4 bytes from a Real*8 and puts them into an Integer*4
PUT--Puts Integer*4 into bits 0-3 of a Real*8
ASIN--Finds arcsin
ATANG--Finds modified arctan

THE LIBRARIES USED IN THE OVERLAY ARE:

STDLUNLIB--Contains binary for all of
above
WFWLTUTIL--System utilities
WFWRUN--Fortran utilities
WFWSOS--System utilities

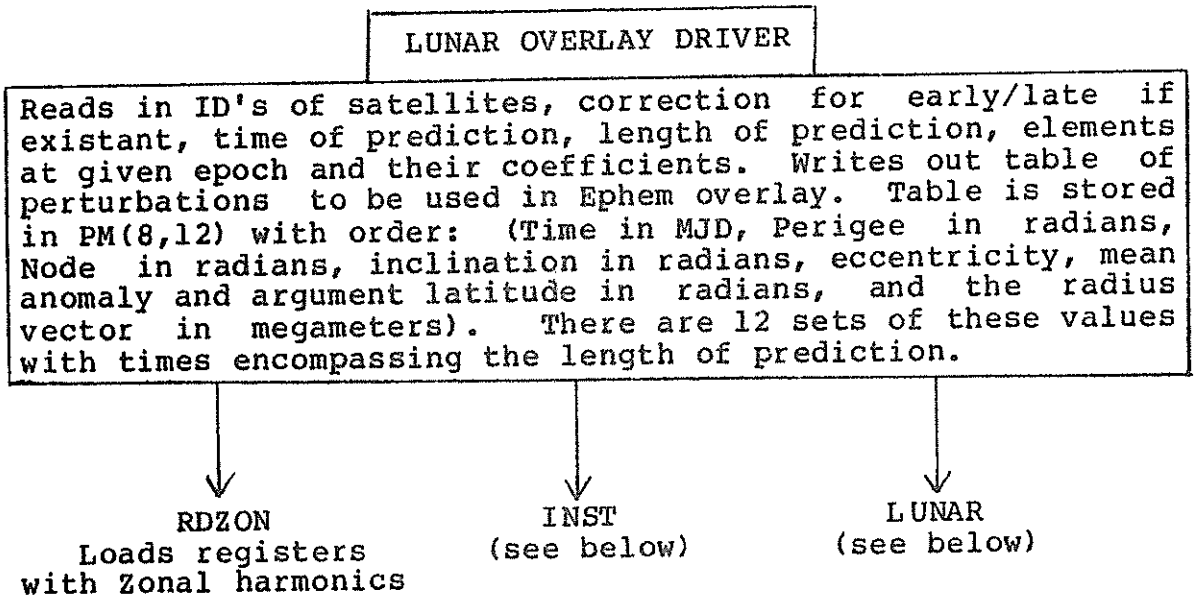
LUNAR OVERLAY DRIVER
Reads in ID's of satellites, correction for early/late if existant, time of prediction, length of prediction, elements at given epoch and their coefficients. Writes out table of perturbations to be used in Ephem overlay. Table is stored in PM(8,12) with order: (Time in MJD, Perigee in radians, Node in radians, inclination in radians, eccentricity, mean anomaly and argument latitude in radians, and the radius vector in megameters). There are 12 sets of these values with times encompassing the length of prediction.
RDZON
Loads registers with Zonal harmonics
INST
(see below)
LUNAR
(see below)

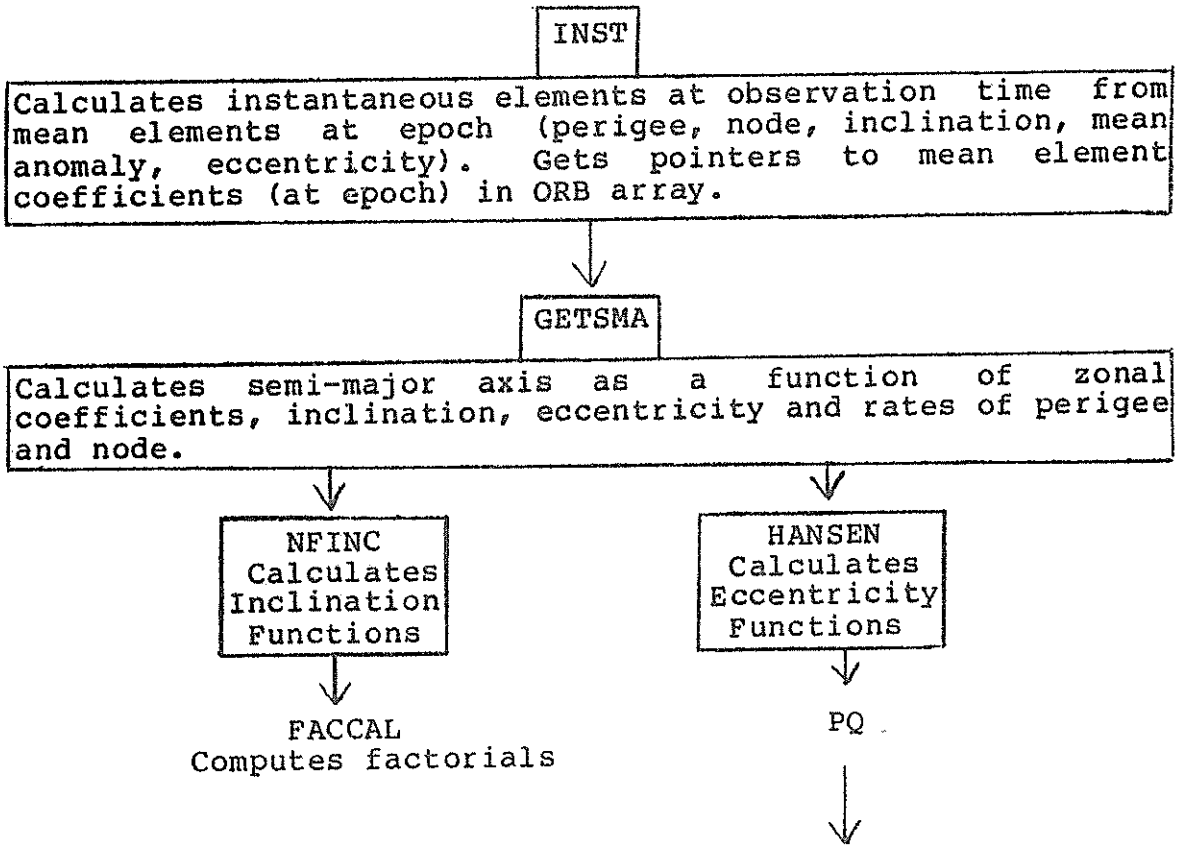
INST
Calculates instantaneous elements at observation time from mean elements at epoch (perigee, node, inclination, mean anomaly, eccentricity). Gets pointers to mean element coefficients (at epoch) in ORB array.
GETSMA
Calculates semi-major axis as a function of zonal coefficients, inclination, eccentricity and rates of perigee and node.
NFINC
Calculates Inclination Functions
HANSEN
Calculates Eccentricity Functions
FACCAL
Computes factorials
PQ

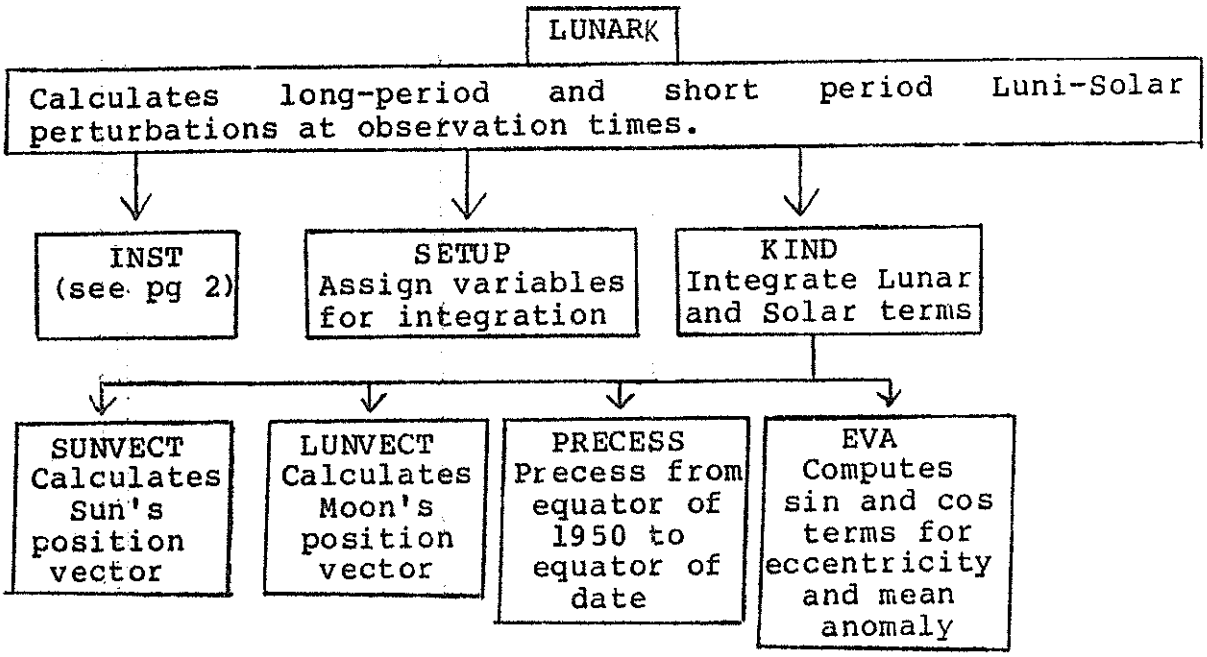
LUNARK
Calculates long-period and short period Luni-Solar perturbations at observation times.
INST
(see pg 2)
SETUP
Assign variables for integration
KIND
Integrate Lunar and Solar terms
SUNVECT
Calculates Sun's position vector
LUNVECT
Calculates Moon's position vector
PRECESS
Precess from equator of 1950 to equator of date
EVA
Computes sin and cos terms for eccentricity and mean anomaly

A REVIEW OF NETWORK DATA HANDLING PROCEDURES

J. H. LATIMER, J. M. THORP,
D. R. HANLON, G. E. GULLAHORN

SMITHSONIAN ASTROPHYSICAL OBSERVATORY

ABSTRACT

We review communications formats for ranging data, and data handling and techniques. Examples of code used for producing or reading various data types are machine-accessible.

DATA FLOW

Network Data handling today is concerned with a variety of data paths and data types. The so-called Quick-Look data cycle is in reality a complex of three information paths which help maintain orbits for a vital network.

The first path is the flow of acquisition ephemerides from central computing facilities to field sites. These data have evolved from centrally-computed pointing angle lists teletyped in lengthy messages to rather brief trajectory descriptions, either Keplerian elements, or IRVs (Inter-Range Vectors). This evolution was made possible by the advent of mini-computers which were placed at field sites.

The second path is the return of a sampling of observational data to the computing center for ephemeris maintenance and data quality monitoring. To be effective, the data must be timely and accurate, yet to be efficient, the data must be evenly sampled and the message format must be reasonably concise.

The third and final path is that used to feed back quality control information to site personnel. Particularly some of the systematic errors can be very subtle and difficult to spot with the information normally available at a remote site. Range biases or epoch timing biases are naturally noticed more readily at a central computing facility. Speed of detection and rectification of such problems is important in order to avoid contamination of large quantities of data.

Final Data

Having organized a Quick-Look data processing cycle to maintain tracking orbits, we must take care to process the complete and final data set for dissemination to the scientific community in as careful a manner as possible. Our problem will tend not to be speed so much as the large quantity of data with which we must contend. The data processing can go much smoother if reasonable data representation is adopted, and of course, submission of data to a data bank such as the National Space Science Data Center run by NASA/Goddard for archiving and distribution requires well understood standard formats.

DATA FORMATS FOR LASER RANGING

The purpose of this section is to document the common data formats in use currently, and to provide code for the creation or transformation of these formats.

Quick-Look

Two well-known Quick-Look formats, the SAO and NASA, are defined in the appendices, and code from the Data General Nova 1200 at SAO field sites which produces 333 data is appended The companion package, a set of routines that are used at SAO's central facility which read 333 data, is listed. These routines also read the NASA Quick-Look format.

Intermediate

At SAO we have two forms of intermediate data representation, for two very different reasons. Because of the large investment in the GRIPE orbital program its coded observation format (known as the DOI format) is retained for use by this program. One advantage of retaining this format was the capability of representing very old data so that long time-span analyses could be undertaken without the

problems of data transformation or program code modification.

Two years ago we adapted to a new computer and in the process of conversion we introduced a machine-specific binary format closely related to the DOI format, but more efficient for data processing (sorting, selection, performing I/O). We treat as utilities those packages which transform from coded representation to binary and vice versa.

Both internal formats are defined in the appendix, and Fortran code is provided for the SAO & NASA Quick-Look to binary transformation and for the SAO final log data to binary transformation. Code is also provided for binary to SEASAT coded, and to DOI coded transformation.

Final

There are two formats in use for representing final data for archiving and distribution. These are the binary and coded formats used by the National Space Sciences Data Center at NASA/GSFC. The coded format is known as the SEASAT format and is broken down in the appendix, and an example of code to produce this format is provided separately. A problem that users of NASA binary data can have is the use of this data on byte-oriented machines such as the DEC VAX. In the code portion of this paper we provide NASABIN which is a utility to transform NASA binary data to SAO internal binary format.

DATA REVIEW PROCEDURES

The most powerful information that a central facility can provide to a remote site is just that information unavailable at the remote site, that is, how well data fits when combined with a global data set in an orbit determination. At SAO we have designed a procedure which does this in a systematic way. Our implementation relies on a post-processor run subsequently to orbit determinations. This post processor reads a file of intermediate information left by the orbit program, and thus has essential information as it existed after the final iterative orbit estimation. In particular, range residuals are available, and partial derivatives to aid in the following simple computation.

The procedure considers each pass from a station individually, and makes a least squares solution for two parameters: a systematic range bias for the pass and a systematic epoch timing bias. This simple procedure builds upon the complicated orbital information already contained in the range residuals from the final orbit estimation process, and we can obtain very reliable noise estimates when there are no large biases present or oscillations in residuals caused by poor orbital modelling. In addition, the estimates of range and time biases can be interpreted. When they are small, there is no problem, as they reflect only the residual long wavelength uncertainties in the orbit modelling process. When they are large, it is indicative of either some defect in the model, such as station coordinates, or error in processing of the data, or real data problems or equipment malfunction.

At SAO all data are reviewed each week and cooperating sites are supplied with comments and interpretation of the post-processor printout. The appendix contains a few examples of these runs showing the summary listings and the individual scatter plots and histograms.

ACKNOWLEDGEMENT

This work was supported by Grant NGR 09-015-002 from the National Aeronautics and Space Administration

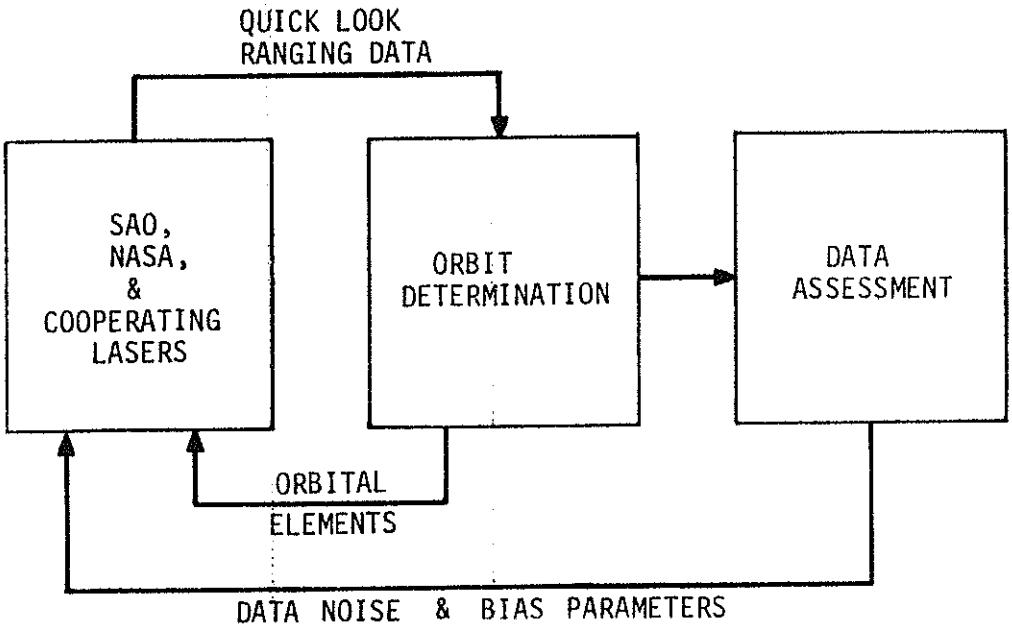

Figure 1.
Network data flow chart.

APPENDICES

SAO QUICK LOOK FORMAT

The SAO laser QL data format is shown below The format consists of five parts:

1. The seven characters "..LASER"
2. Station header line (words 1 through 3)
3. Pass header line (words 4 through 9)
4. Data lines (words 10 through 14 in each line)
5. The three characters "END".

Each word (1 through 14) has five decimal characters. Words are separated by one space. An explanation of each word follows:

WORD	CHARACTER	EXPLANATION
1	1 through 5	Always 33333
2	1 through 4	Station no.
2	5 and	
3	1	Year of century
3	2,3	Month of year
3	4,5	Day of month
4	1 through 5 and	
5	1,2	COSPAR Satellite ID
5	3	Sky/Shadow code for first point of pass: 0 => night, satellite illuminated; 1 => night, satellite in shadow; 2 => day
5	4,5	Relative humidity in percent
6	1	Sign of temperature. 0 => positive, 1 => negative
6	2 through 4	Temperature in units of 0.1 degree Celsius
6	5	Unused, always zero
7	1 through 4	Barometric pressure in millibars
7	5 and	
8	1 through 5	Pre-pass calibration average in units of 0.1 nanosec
9	1 through 5	Post-pass calibration average with ten thousand nanosec digit implied equal to that of Pre-pass
10	1,2	Epoch of pulse transmission hours (UT)
10	3,4	Minutes
10	5 and	

11	1	Seconds
11	2 through 5 and	
12	1,2	Microseconds
12	3,4	Check word
12	5	Confidence: 0 => probably good; 1 => probably bad
13	1 through 5 and	
14	1 through 5	Two-way range in 0.1 nanoseconds

The seven characters "..LASER" appear once at the beginning of each data transmission. The station header line is repeated for each different day of data within the transmission message. A pass header line begins each pass. Each data transmission ends with the three characters "END".

Sample 333 Quick Look laser data message

..LASER

Word 1	2	3			
33333	79438	01013			
Word 4	**5**	**6**	**7**	**8**	**9**
76039	01099	10500	09141	28659	28661
Word 10	**11**	**12**	**13**	**14**	
14311	49407	96610	05422	23382	

END

NASA Quicklook Format

Character	Description
1	"CR"
2	"CR"
3	"LF"
4	"1"
5	"B"
6	"B"
7-10	SIC (Spacecraft Identification Code)
11-12	VID
13-14	STATION ID (from STDN 724)
15-16	MOVE NUMBER - Sequence from birth
17	MOUNT TYPE "0" = AZ/EL "1" = X/Y
18	LASER/LAST FRAME INDICATOR "0" = Prime Laser/Not Last Frame "1" = Backup Laser/Not Last Frame "4" = Prime Laser/Last Frame "5" = Backup Laser/Last Frame
19	MODE "0" = Program Track "1" = AUTOTRACK (not currently available).
20	"SPACE"
21-25	WAVELENGTH in nm
26	"SPACE"
27-28	YEAR (mod 100)
29-31	DAY OF YEAR
32-36	SECONDS OF DAY
37-42	MICROSECONDS OF SECONDS
43	"SPACE"
44-49	ANGLE 1 (X or AZ) in 001 For X angle: If plus, then lead character will be a zero; if minus, then lead character will be minus sign. For AZ angle: Lead character will be 0, 1, 2, or 3.
50	"SPACE"
51-56	ANGLE 2 (Y or EL) in .001 In plus, then lead character will be a zero. Otherwise there will be a minus sign.

Character	Description
57	"SPACE"
58-69	RANGE (roundtrip time) in .01 nsec.
70-72	"SPACES"
73	"4"
74	"F"
75	"F"

NOTE: All values in quotes are constants and should be replaced by either their ASCII or BAUDOT representations (depending on whether it is 8 or 5 level).

DOI Data Card Format

This document describes the observation card format as read by GRIPE.

Field	Cols.	Description
1	1-7	Cospar Satellite Identification
2	8-12	Sequence Number
3	13-17	Station Number
4	18-23	Date of Observation
	18-19	year
	20-21	month
	22-23	day
5	24-33	Time designation
	24-25	hour
	26-27	minute
	28-29	second
	30-36	fraction of seconds to .1 microsec
6	37-46	observed range in meters, to .01 meters (xxxxxxxx.xx) or 2-way range in nano-seconds, to .1 nanosec. (xxxxxxxxx.xx)
7	49-52	refraction correction, to .01 meters (xx.xx) to be subtracted from range. This value, if present, may or may not have already been applied to the range (see columns 57&58)
8	53-58	Index Codes

Field	Cols.	Description
9	53	Time-precise index Code — Standard error in timing σ_t 0 — no estimates 1 — $\sigma_t \leq .003$sec 2 — $.003 < \sigma_t \leq .002$ 3 — $.002 < \sigma_t \leq .005$ 4 — $.005 < \sigma_t \leq .02$ 5 — $.02 < \sigma_t \leq .05$ 6 — $.05 < \sigma_t \leq .2$ 7 — $.2 < \sigma_t \leq .5$ 8 — $.5 < \sigma_t \leq 2.0$ 9 — $2.0 < \sigma_t$
	54-55	Standard Deviation a) either in meters and tenths of meters (or n.s and .1 n.s) (if col 54-55 < 25) or b) x, where x = 25 (log + 3) and = weight in meters (if col 54-55 > 25)
	56	Observation type index: always 8 for laser range
	57	Epoch System/Corrections Applied Index If col 56 = 8 (range obs.), then column 57, in conjunction with column 58, determines the time of the data taken and the corrections (refraction and center of mass) that have been applied and/or given

57	laser type	epoch	ref. corr	center of mass	weather info
0	A	trans	none	none	given
1	B	rcvd	given	none	given
2	new B	rcvd	given	given	given
3	old D	at sat.	applied	none	optional
4	new D	trans	see 58	see 58	given
5	E	trans	see 58	see 58	given

Field	Cols.	Description
	58	For col 56 = 8 (range in meters or nanosec) it gives obs. units and correction applied information. Values 1-7 refer to new laser D and E only. Values 8 & 9 refer to laser A, B and old D.

58	Explanation
1	one way range, in meters, not corrected for atmospheric refraction or spacecraft center of mass
2	one way range, in meters, corrected for atmospheric refraction and spacecraft center of mass
3	two way range, in nanoseconds, not corrected for atmospheric refraction or spacecraft center of mass
4	two way range, in nanoseconds, atmospheric refraction and spacecraft center of mass given, neither applied
5	two way range, in nanoseconds, atmospheric refraction and spacecraft center of mass corrections given, and applied
7	one way range, in meters, refraction correction and spacecraft center of mass corrections given, neither applied
8	one way range, in meters, see column 57 for atmospheric refraction and spacecraft center of mass correction information

Field	Cols.	Description
9	59-62	Calibration Stability
	59-61	Difference between pre and post calibration (absolute value) in nanoseconds included when code in column 62 is 2; no estimate otherwise
	59	tens
	60	units
	61	tenths
	62	Calibration index

Code no.	Explanation
2	Pulse processer system-pre & post
3	Pulse processer system-only one calibration
4	Pulse processer system-no pre or post calibration

10	63-66	Spacecraft center of mass correction
	63	Blank
	64-66	Spacecraft corr. to .01 meters to be added to range. This value, if present, may or may not have already been applied to the range, depending on cols. 57 and 58.
11	67-76	Weather Data
	67-70	Pressure (millibars)
	71-72	humidity (percent)
	73-76	temperature (Celsius to tenths)
12	77-81	Elevation angle to .001 degree
13	82-94	Predicted range
	82	blank
	83-92	2-way range to .1 n.s.
	93-94	blank

Field	Cols.	Description
14	95-100	Azimuth Angle to .001 degree
15	101-103	Speed of Light Code
	101	blank
	102-103	= 00 if c = 2.997925E10 cm/sec was used in reduction = 01 if c = 2.99792458E10 cm/sec was used in reduction
16	104-105	Range noise - given as 25 (log y + 3) where y = range noise in meters
17	106-107	Estimated Range Error - given as 25 (log z + 3) where z = estimated range bias in meters

SAO INTERNAL BINARY FORMAT FOR LASER OBSERVATIONS

ITEM 1 Satellite Identification (I*4)
ITEM 2 Observation Sequence no. and REJECTION FLAG (I*4)
This number, when negative, indicates that the observation has been rejected.
ITEM 3 Station no. (I*2)
ITEM 4 Modified Julian Date of Observation (I*4)
ITEM 5 Fractional part of Day of Observation (R*8)
ITEM 6 Type of Observation:
0 = end of pass
8 = laser observation
18 = laser observation; processed by GRIPE
ITEM 7 Observed Range (R*8) (Units depend on items 11, 12 - see GRIPE Manual)
ITEM 8 Refraction Correction in meters (R*4)
ITEM 9 Time precision (Standard Error) in seconds (R*4)
ITEM 10 Range Precision (Standard Error) in meters (R*4)
ITEM 11 Epoch System/Corrections Applied Index (identically same meaning as col. 57 of DOI format in GRIPE manual) (I*2)
ITEM 12 Observation Units/Corrections Applied Index (identically same as col. 58 of DOI format in GRIPE manual) (I*2)
ITEM 13 Calibration Stability (Pre-calibration minus Post-calibration in nanoseconds when Calibration Index = 2, Null otherwise) (r*4)
ITEM 14 Calibration Index(Same as col. 62 of DOI format) (I*2)
ITEM 15 Center of Mass correction in meters (r*4)
ITEM 16 Atmospheric pressure in millibars (R*4)
ITEM 17 Percent Relative Humidity (R*4)
ITEM 18 Atmospheric temperature in degrees Celsius (R*4)
ITEM 19 Predicted Elevation Angle in degrees (R*4)
ITEM 20 Predicted Range (Two-way) in nanoseconds (R*8)
ITEM 21 Predicted Azimuth Angle in degrees (R*4)
ITEM 22 Speed of Light Index (same as col. 102-103 of DOI format) (I*2)
ITEM 23 Estimated Range Noise in meters (R*4)
ITEM 24 Estimated Range Bias in meters (R*4)
ITEM 25 Year of Observation minus 1900 (I*2)
ITEM 26 Month of Observation (I*2)
ITEM 27 Day of Observation (I*2)
ITEM 28 Hour of day of Observation (I*2)
ITEM 29 Minute of hour of Observation (I*2)
ITEM 30 Seconds of minute of Observation (R*8)
ITEM 31 Pass Sequence Number (Negative for Quick Look, Positive for Final) (I*2)
ITEM 32 Twelve bytes of zeroes reserved for future expansion

TOTAL OBSERVATION RECORD LENGTH = 128 (8-bit) bytes

SAO INTERNAL BINARY FORMAT FOR LASER OBSERVATIONS

INDEXING SCHEME

ITEM NUMBER	VAX MNEMONIC	FIRST BYTE	LAST BYTE (= 8 bits)
1	I*4	1	4
2	I*4	5	8
3	I*2	9	10
4	I*4	11	14
5	R*8	15	22
6	I*2	23	24
7	R*8	25	32
8	R*4	33	36
9	R*4	37	40
10	r*4	41	44
11	I*2	45	46
12	I*2	47	48
13	R*4	49	52
14	I*2	53	54
15	R*4	55	58
16	R*4	59	62
17	R*4	63	66
18	R*4	67	70
19	R*4	71	74
20	R*8	75	82
21	R*4	83	86
22	I*2	87	88
23	R*4	89	92
24	R*4	93	96
25	I*2	97	98
26	I*2	99	100
27	I*2	101	102
28	I*2	103	104
29	I*2	105	106
30	R*8	107	114
31	I*2	115	116
32	12 Bytes	117	128

Sample implementation of reading the new internal SAO laser observation record:

Having declared:
INTEGER*4 SATELLITE, OBSNO, MJD
INTEGER*2 STATION, TYPE, DUMMY(52)
DOUBLE PRECISION FRACTION
we can then read any type of data, laser or otherwise:

```
READ (filespec) SATELLITE, OBSNO, STATION, MJD, FRACTION, TYPE, DUMMY
                  (INT)    (INT)   (INT)   (INT)   (DP)     (INT) (INT)
```

Then, if TYPE = 8 (indicating a laser observation) the following equivalences will apply:

LASER OBS WORD	DUMMY
7	1
8	5
9	7
10	9
11	11
12	12
13	13
14	15
15	16
16	18
17	20
18	22
19	24

LASER OBS WORD	DUMMY
20	26
21	30
22	32
23	33
24	35
25	37
26	38
27	39
28	40
29	41
30	42
31	46

where LASER OBS WORDS 7, 20, and 30 are DOUBLE PRECISION, and LASER OBS WORDS 11, 12, 14, 22, 25, 26, 27, 28 and 31 are short integers (I*2), and the remaining LASER OBS WORDS are (R*4) single precision floating point numbers.

NASA BINARY FORMAT

The FORTRAN variable types used in this format description are:

I*2 - Half-word integer
I - Single word Integer
R - Single word Floating Point
DP - Double word Floating Point

Description of Bytes 1-28 for all measurement types.

Bytes	FORTRAN Variable Type	Description
1-4	I	Satellite ID
5-6	I*2	Measurement Type 20 = Laser 64-69 = X-Y Angles (North-South) 68 = Laser 70-79 = Azimuth and Elevation Angles 70 = Laser
7-8	I*2	Time System Indicator (nm) n value description 1 Satellite Transponder/(reflector) Transmitter Time m value description 3 UTC
9-12	I	Station Number
13-16	I	Preprocessing Indicators/Report The preprocessing indicators are bit switches packed into a single 32 bit word. The rightmost bit (bit 31) is of lowest order and the leftmost bit (bit 0) is of highest order.

Bytes	FORTRAN Variable Type	Description

The preprocessing bits are configured as follows:

Bits	Value	Description
0		This bit should always be zero filled
3		Beacon Activity Indicator (types 10-14)
	0	Beacon Inactive or No Beacon
	1 or	Beacon Active Center of Mass Offset Correction Indicator (range, range rate, altimeter)
	0	Data corrected for offset
	1	Data uncorrected for offset
		Unused Equator Designation (types 10-14)
5-6		Date of Equator and Equinox (types 10-14)
		Speed of Light Indicator, (Range, Range Rate, and Altimeter)
	0	2.997925 x 10 meters/sec
	1	2.997925 x 10 meters/sec
	2	2.997925 x 10 meters/sec
	3	2.99792458 x 10 meters/sec

Bytes	FORTRAN Variable Type	Description		
		10-12		Tropospheric Refraction (all but Types 10-14)
			0	Data has been corrected and meteorological data not present
			1	Data has not been corrected
			2	Data has been corrected using the correction formulas for international laser data. Correction value is for zero zenith
			3	Data has not been corrected. Correction Value is for zero zenith.
			4	Data has been corrected and meteorological data is present.
			5	Data has not been corrected and meteorological data is present.
		13		Ionospheric Refraction (all but Types 10-14)
			0	Data has been corrected
			1	Data has not been corrected
		15		Antenna Axis Displacement (Types 20-29)
			0	Data has been corrected (or no correction required)
			1	Data has not been corrected (correction is required)
		16-17		Receiever Mount Type (all but Types 10-14, and Types 38-59)
			1	X-Y (North-South)
			2	Azimuth-Elevation

Bytes	FORTRAN Variable Type	Description
		18-19 Transmitter Mount Type (all but Types 10-14, and Types 38-59)
		1 X-Y (North-South)
		2 Azimuth-Elevation
17-20	I	Modified Julian Date (MJD) of observation. JD = MJD + 2400000.5
21-28	DP	Fraction of Day Past Midnight (GMT)
29-36	DP	Observation Value in Radians for Right Ascension, or Hour Angle, or Azimuth, or X-Angle
37-44	DP	Observation Value in Radians for Declination, or Elevation, or Y-Angle
Bytes 29-68 for Range and Range Rate Measurements (Types 20-39)		
29-36	DP	Observation Value in Meters for Range (Types 20-29) and Meters/Second for Range Rates (Types 30-39)
49-52	I	Average Range Rate Data (Types 30, 33, 34, and 38: Counting Interval in Microseconds.
		Laser Data: Tropospheric Refraction Correction in Same Units as Observation.
53-56	R	Meteorological Data
57-60	R	Ionospheric Refraction Correction in Same Units as Observation
65-68	R	Other than Laser Data: Transmitter Antenna Axis Displacement in Meters.
		Laser Data; Correction to Spacecraft Center of Mass.

SEASAT FORMAT FOR LASER RANGING OBSERVATIONS
A 90 character card image representation.

Column	Subset	Description
1-7		Satellite ID
8-9		Always 20 for laser ranging data
10-11		Time System Indicator
	10	0 => Ground Received Time
		1 => Satellite Transponder/Transmitter Time
		2 => Satellite Receiver Time
	11	0 => UT-0
		1 => UT-1
		2 => UT-2
		3 => UT-C
		4 => A.1
		5 => A.3 (AT BIH)
		6 => AS (SAO)
12-16		Station ID
17-32		GMT of Observation
	17-18	Year of century
	19-21	Day of year
	22-26	Time of day (Seconds from midnight GMT)
	27-32	Fractional part of seconds in units of microsec.
33-35		Preprocessing Indicators
	33	0 => Data has been corrected for tropospheric refraction.
		1 => Data has not been corrected for tropospheric refraction.
		2 => Data has been corrected for tropospheric refraction, using the correction formulae for international laser data (see cols. 76-80).
		3 => Data not corrected for tropospheric refraction. Cols. 76-80 contain coefficient for use with international laser formulae.
		4 or 5 => Cols. 57-66 will contain meteorological data.
	35	Data (0 => has; 1 => has not) been corrected for transponder delay effects.
36-54		Observation data
	36-45	Range in km units
	46-54	Fraction of km Range in units of micrometers
55-56		Preprocessing Indicators
	55	Preprocessing report (Spare, always 0)
	56	Transponder type
		1 => coherent; 2 => non-coherent
57-66		Meteorological data if col. 34 contains a 4 or 5.
	57-60	Surface pressure in millibars
	61-63	Surface temperature in degrees Kelvin
	64-66	Relative humidity in percent

69-73	Measurement standard deviation in millimeters
74-75	Not used for laser data
76-80	Tropospheric refraction correction in millimeters or Coefficient of tropospheric refraction international lasers in millimeters (see col. 34)
81	Speed of light indicator 0 => 299792.5 km/s 1 => 299792.458 km/s
82	Center of mass correction application indicator 0 => applied 1 => not applied
83-88	Center of mass correction in millimeters
89-90	Log10 of the standard deviation of the time of observation in microseconds.

SAMPLE DATA REVIEW OUTPUT

7090 YARRAGADEE														
7603901	39	39	39	40	2	38	40	40	40	40	39	40		
7110 MONUMNT PK														
7603901	40	40	2	40	39	37	39	40	1	40	1			
7120 MAUI														
7603901	39	49	44	35	43	39	40	10						
7102 G F S C														
7603901	8													
7112 PLATTEVILL														
7603901	39	39	3	6	39	14	3	11						
7105 GODDARD														
7603901	42	40	32	40	40									
7210 HALEAKALA														
7603901	39	39	38	37	30	39	38	40						
7831 HELWAN														
7603901	10	24	12	13	28									
7833 KOOTWIJK														
7603901	6													
7834 WETTZELL														
7603901	14	22	16	15	18									
7805 METSAHOVI														
7603901	25	16	27											
7943 ORRORAL V														
7603901	39	30	39	23	10									
7907 AREQUIPA														
7603901	38	37	37	1	38	39	36	39	3	33	37	39	34	31
7929 NATAL														
7603901	25	27	27	34	10	38								

pass	site	satellite	mod julian dy	sigma	timebias(msec)		rangebias(M)		good-bad		day	yr	mon	dy	time
1	7090	7603901	44849.074121	0.16	0.049	0.022	-0.021	0.039	39	1	WED	81	SEP	2	146
2	7090	7603901	44849.216864	0.21	-0.339	0.032	-0.691	0.034	39	1	WED	81	SEP	2	512
3	7090	7603901	44849.736898	0.09	-0.267	0.035	0.108	0.054	39	1	WED	81	SEP	2	1741
4	7090	7603901	44854.598912	0.19	-0.029	0.033	-0.536	0.042	40	0	MON	81	SEP	7	1422
5	7090	7603901	44856.630510	0.00	0.000	0.000	0.000	0.000	2	0	WED	81	SEP	9	15 7
6	7090	7603901	44856.656088	0.12	0.571	0.107	-2.004	0.252	38	0	WED	81	SEP	9	1544
7	7090	7603901	44856.782234	0.12	-0.042	0.017	-0.257	0.019	40	0	WED	81	SEP	9	1846
8	7090	7603901	44857.060591	0.22	0.201	0.027	0.270	0.045	40	0	THU	81	SEP	10	127
9	7090	7603901	44857.577604	0.24	-0.167	0.043	-0.091	0.038	40	0	THU	81	SEP	10	1351
10	7090	7603901	44857.721760	0.12	-0.353	0.011	0.114	0.019	40	0	THU	81	SEP	10	1719
11	7090	7603901	44858.005058	0.16	-0.268	0.025	0.315	0.027	39	1	FRI	81	SEP	11	0 7
12	7090	7603901	44858.145116	0.28	-0.108	0.030	-0.060	0.046	40	0	FRI	81	SEP	11	328
13	7110	7603901	44849.157801	1.14	2.336	0.151	12.522	0.187	40	0	WED	81	SEP	2	347
14	7110	7603901	44849.303345	0.86	3.792	0.097	5.350	0.157	40	0	WED	81	SEP	2	716
15	7110	7603901	44849.827674	0.00	0.000	0.000	0.000	0.000	2	38	WED	81	SEP	2	1951
16	7110	7603901	44850.249179	1.17	2.397	0.136	9.109	0.237	40	0	THU	81	SEP	3	558
17	7110	7603901	44856.195510	1.88	2.785	0.180	5.741	0.301	39	1	WED	81	SEP	9	441
18	7110	7603901	44856.349584	0.20	4.045	0.040	-0.849	0.042	37	3	WED	81	SEP	9	823
19	7110	7603901	44857.155058	0.25	0.475	0.079	15.122	0.119	39	1	THU	81	SEP	10	343
20	7110	7603901	44857.283334	1.02	4.223	0.095	4.670	0.162	40	0	THU	81	SEP	10	648
21	7110	7603901	44857.960417	0.00	0.000	0.000	0.000	0.000	1	16	THU	81	SEP	10	23 3
22	7110	7603901	44858.232361	1.19	2.651	0.122	8.392	0.199	40	0	FRI	81	SEP	11	534
23	7110	7603901	44858.759560	0.00	0.000	0.000	0.000	0.000	1	15	FRI	81	SEP	11	1813
24	7120	7603901	44849.301713	0.17	0.624	0.019	-0.027	0.027	39	1	WED	81	SEP	2	714
25	7120	7603901	44849.456100	0.09	-0.183	0.030	0.668	0.053	49	2	WED	81	SEP	2	1056
26	7120	7603901	44851.331760	0.15	-0.319	0.014	-0.331	0.023	44	1	FRI	81	SEP	4	757
27	7120	7603901	44852.280533	0.09	0.647	0.182	-0.146	0.339	35	1	SAT	81	SEP	5	643
28	7120	7603901	44852.428241	0.23	0.170	0.027	-0.063	0.037	43	0	SAT	81	SEP	5	1016
29	7120	7603901	44857.291482	0.12	0.603	0.016	-0.030	0.019	39	1	THU	81	SEP	10	659
30	7120	7603901	44857.432176	0.25	0.314	0.026	-0.358	0.039	40	0	THU	81	SEP	10	1022
31	7120	7603901	44858.247338	0.16	-0.030	0.132	-1.019	0.066	10	3	FRI	81	SEP	11	556
32	7102	7603901	44858.083617	3.99	0.626	1.404	-2.384	2.162	8	32	FRI	81	SEP	11	2 0
33	7112	7603901	44849.164294	0.86	1.229	0.128	12.353	0.199	39	0	WED	81	SEP	2	356
34	7112	7603901	44849.306794	0.32	3.840	0.067	4.626	0.053	39	1	WED	81	SEP	2	721
35	7112	7603901	44851.854028	0.00	0.000	0.000	0.000	0.000	3	3	FRI	81	SEP	4	2029
36	7112	7603901	44855.776922	19.83	-28.168	33.402	-16.530	21.475	6	12	TUE	81	SEP	8	1838
37	7112	7603901	44856.209595	0.33	0.739	0.092	13.685	0.143	39	1	WED	81	SEP	9	5 1
38	7112	7603901	44858.751262	9.11	-2.499	4.695	6.775	3.699	14	16	FRI	81	SEP	11	18 1
39	7112	7603901	44858.769433	0.00	0.000	0.000	0.000	0.000	3	7	FRI	81	SEP	11	1827
40	7112	7603901	44858.904306	17.03	-7.244	11.142	10.616	18.741	11	21	FRI	81	SEP	11	2142
41	7105	7603901	44856.191379	0.26	0.160	0.037	0.288	0.046	42	0	WED	81	SEP	9	435
42	7105	7603901	44857.132664	0.18	1.112	0.019	-0.575	0.039	40	0	THU	81	SEP	10	311
43	7105	7603901	44857.658023	0.06	-0.334	0.025	-1.823	0.011	32	1	THU	81	SEP	10	1547
44	7105	7603901	44858.079921	0.05	0.396	0.006	-1.097	0.009	40	0	FRI	81	SEP	11	155
45	7105	7603901	44858.230037	0.08	0.527	0.018	1.304	0.013	40	0	FRI	81	SEP	11	531
46	7210	7603901	44849.303091	0.55	-0.016	0.093	1.176	0.110	39	1	WED	81	SEP	2	716
47	7210	7603901	44849.447396	0.48	0.324	0.057	-0.421	0.077	39	1	WED	81	SEP	2	1044
48	7210	7603901	44851.335429	0.74	-0.715	0.095	0.008	0.138	38	2	FRI	81	SEP	4	8 3

49	7210	7603901	44851.485463	0.51	0.063	0.115	0.847	0.091	37	3	FRI	81	SEP	4	1139
50	7210	7603901	44852.433091	0.48	0.390	0.076	-0.764	0.114	30	10	SAT	81	SEP	5	1023
51	7210	7603901	44856.342836	0.71	-0.615	0.081	0.147	0.136	39	1	WED	81	SEP	9	813
52	7210	7603901	44857.290220	0.23	0.243	0.044	1.194	0.045	38	1	THU	81	SEP	10	657
53	7210	7603901	44857.434838	0.40	0.136	0.053	-0.650	0.064	40	0	THU	81	SEP	10	1026
54	7831	7603901	44852.759723	0.23	1.968	0.096	-8.885	0.073	10	0	SAT	81	SEP	5	1814
55	7831	7603901	44852.902315	0.62	1.136	0.280	1.049	0.378	24	4	SAT	81	SEP	5	2139
56	7831	7603901	44853.843403	0.25	1.890	0.218	4.079	0.424	12	0	SUN	81	SEP	6	2014
57	7831	7603901	44854.790463	0.23	1.603	0.053	-1.371	0.064	13	1	MON	81	SEP	7	1858
58	7831	7603901	44855.878264	1.05	2.506	0.351	7.328	0.533	28	0	TUE	81	SEP	8	21 4
59	7833	7603901	44850.887640	0.42	0.182	0.342	1.475	0.177	6	0	THU	81	SEP	3	2118
60	7834	7603901	44851.819096	0.24	-0.130	0.140	-0.483	0.259	14	2	FRI	81	SEP	4	1939
61	7834	7603901	44851.970002	0.22	0.672	0.273	1.805	0.401	22	1	FRI	81	SEP	4	2316
62	7834	7603901	44854.807093	0.24	-0.265	0.193	0.196	0.112	16	0	MON	81	SEP	7	1922
63	7834	7603901	44854.948875	0.27	-1.570	0.667	-1.909	0.786	15	0	MON	81	SEP	7	2246
64	7834	7603901	44857.921731	0.26	0.230	0.249	0.149	0.366	18	0	THU	81	SEP	10	22 7
65	7805	7603901	44851.819786	1.95	-0.060	0.263	12.470	0.393	25	0	FRI	81	SEP	4	1940
66	7805	7603901	44853.854685	3.12	-0.606	0.548	12.779	0.811	16	0	SUN	81	SEP	6	2030
67	7805	7603901	44854.796003	2.73	0.183	0.310	9.234	0.526	27	0	MON	81	SEP	7	19 6
68	7943	7603901	44854.592446	0.37	0.251	0.043	0.248	0.071	39	1	MON	81	SEP	7	1413
69	7943	7603901	44854.752865	0.52	-0.974	0.314	0.957	0.515	30	0	MON	81	SEP	7	18 4
70	7943	7603901	44855.535329	0.47	0.942	0.046	0.387	0.077	39	1	TUE	81	SEP	8	1250
71	7943	7603901	44855.690365	0.37	0.271	0.105	0.207	0.080	23	0	TUE	81	SEP	8	1634
72	7943	7603901	44857.564755	0.92	0.146	0.315	0.090	0.586	10	0	THU	81	SEP	10	1333
73	7907	7603901	44852.098522	0.31	-0.083	0.033	-0.123	0.050	38	2	SAT	81	SEP	5	221
74	7907	7603901	44852.246438	0.41	-0.047	0.048	0.546	0.090	37	3	SAT	81	SEP	5	554
75	7907	7603901	44853.205641	0.72	-0.490	0.167	-0.165	0.386	37	2	SUN	81	SEP	6	456
76	7907	7603901	44853.634807	0.00	0.000	0.000	0.000	0.000	1	0	SUN	81	SEP	6	1514
77	7907	7603901	44854.138886	0.38	-0.240	0.056	-0.022	0.071	38	2	MON	81	SEP	7	319
78	7907	7603901	44854.290712	0.53	-0.448	0.121	0.712	0.170	39	1	MON	81	SEP	7	658
79	7907	7603901	44855.077605	0.48	-0.040	0.079	0.342	0.102	36	4	TUE	81	SEP	8	151
80	7907	7603901	44855.221960	0.40	0.070	0.049	0.196	0.084	39	1	TUE	81	SEP	8	519
81	7907	7603901	44856.167188	0.00	0.000	0.000	0.000	0.000	3	0	WED	81	SEP	9	4 0
82	7907	7603901	44856.181591	0.33	-0.495	0.056	0.113	0.129	33	4	WED	81	SEP	9	421
83	7907	7603901	44856.321353	0.67	-0.982	0.171	0.930	0.149	37	2	WED	81	SEP	9	742
84	7907	7603901	44857.108158	0.45	0.095	0.047	0.154	0.083	39	2	THU	81	SEP	10	235
85	7907	7603901	44858.057550	0.54	-0.687	0.105	0.286	0.100	34	6	FRI	81	SEP	11	122
86	7907	7603901	44858.195137	0.60	-0.402	0.064	0.397	0.167	31	9	FRI	81	SEP	11	440
87	7929	7603901	44850.067101	0.51	-0.381	0.066	-0.032	0.104	25	15	THU	81	SEP	3	136
88	7929	7603901	44852.104602	0.37	-0.121	0.116	-0.307	0.094	27	13	SAT	81	SEP	5	230
89	7929	7603901	44853.991580	0.36	-0.012	0.101	0.967	0.070	27	2	SUN	81	SEP	6	2347
90	7929	7603901	44854.138802	0.65	-0.262	0.120	-0.356	0.111	34	6	MON	81	SEP	7	319
91	7929	7603901	44855.077864	0.56	-0.325	0.425	-1.102	0.864	10	0	TUE	81	SEP	8	152
92	7929	7603901	44856.022828	0.39	-0.151	0.074	0.635	0.066	38	2	WED	81	SEP	9	032

92 PASSES 2700 "GOOD" OBS 286 "BAD" OBS

```
* * * *
station 7831   weight  1.   satellite 7603901  from   81   9   5   44852.9023152   to      44852.9143985  POLE SOLUTION   HELWAN
ITERATIONS  2 3-TIMES A PRIORI SIGMA  0.2E-04 A PRIORI SCALE  0.000E+00 OBS REJECT FLAG 0-AUTO,1-MANUAL 0  DELTA GM/2GM  0.000E+00
SOLUTION VECTOR (DAYS,MEGAMETERS)    0.4586E-08 -0.1533E-06      ITERATION  1
SIGMA IS   1.519     1.457 RMS(M)
SOLUTION VECTOR (DAYS,MEGAMETERS)    0.8557E-08  0.1203E-05      ITERATION  2
 21 39 20.036       -0.178    1.  41.   -1.19     1
 21 39 32.036       -0.706    1.  41.   -1.69     2
 21 39 56.036        1.028    1.  42.    0.09     3
 21 40  8.036        1.420    1.  43.    0.51     4
 21 40 12.036       -0.826    1.  43.   -1.72     5
 21 40 36.036        0.141    1.  44.   -0.70     6
 21 40 52.036        0.018    1.  44.   -0.79     7
 21 41 36.036        0.019    1.  46.   -0.68     8
 21 41 44.036       -1.554    1.  46.   -2.24     9
 21 41 52.036        0.016    1.  46.   -0.65    10
 21 41 56.036       -0.246    1.  46.   -0.90    11
 21 42 12.036       -0.027    1.  47.   -0.64    12
 21 42 44.036       -0.003    1.  48.   -0.54    13
 21 44  4.036        0.782    1.  50.    0.45    14
 21 44 16.036        0.036    1.  51.   -0.26    15
 21 44 20.036       -0.559    1.  51.   -0.84    16
 21 44 36.036       -0.068    1.  51.   -0.31    17
 21 45  8.036        0.263    1.  52.    0.11    18
 21 45 52.036        0.467    1.  53.    0.44    19
 21 46 36.036       -0.010    1.  54.    0.09    20
 21 47 16.036        0.595    1.  55.    0.81    21
 21 47 32.036       -7.027    0.  56.   -6.77    22
 21 48 12.036       -0.039    1.  56.    0.34    23
 21 49 56.037       -0.289    1.  58.    0.40    24
 21 50 28.037       -0.278    1.  58.    0.51    25
 21 52 32.037      -46.825    0.  58.  -45.65    26-
 21 54  0.038      -66.657    0.  58.  -65.22    27-
 21 56 44.027      -96.862    0.  55.  -94.94    28-
*     7831         7603901
*    81  9  5     21 39 20.036
*    28 POINTS    24 ACCEPTED     4 REJECTED
*  RANGE  NOISE =    0.622 RMS =    0.596
*  TIME  OFFSET =       1.136 +OR-    0.280 MSEC
*  RANGE OFFSET =       1.049 +OR-    0.378 METER
                                     SIGMA
```

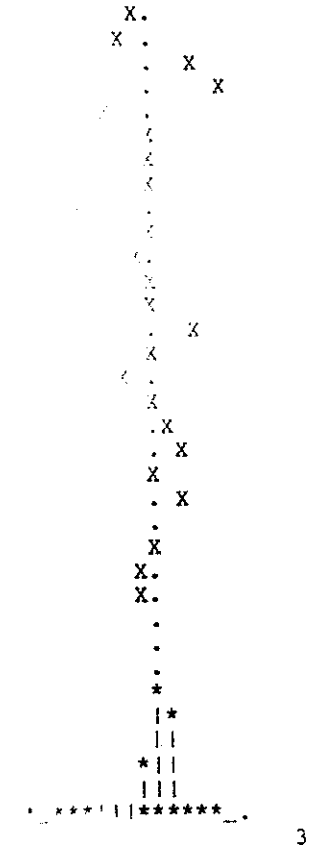

```
* * * *
station 7834   weight  1.   satellite 7603901  from    81   9   7   44854.8070929   to      44854.8115229  POLE SOLUTION   WETTZELL
ITERATIONS  2 3-TIMES A PRIORI SIGMA  0.2E-04 A PRIORI SCALE  0.000E+00 OBS REJECT FLAG 0-AUTO,1-MANUAL 0  DELTA GM/2GM  0.000E+00
SOLUTION VECTOR (DAYS,MEGAMETERS)  -0.3067E-08  0.1963E-06      ITERATION  1
SIGMA IS   0.235     0.220 RMS(M)
SOLUTION VECTOR (DAYS,MEGAMETERS)  -0.3463E-19 -0.1933E-16      ITERATION  2
 19 22 12.828      -0.380   1.  67.  -0.16    1
 19 22 36.079       0.137   1.  67.   0.34    2
 19 23 38.827       0.432   1.  67.   0.58    3
 19 23 49.577       0.019   1.  67.   0.16    4
 19 24  6.827      -0.115   1.  66.   0.01    5
 19 25  2.826       0.275   1.  65.   0.35    6
 19 25 13.076      -0.052   1.  65.   0.02    7
 19 25 28.078       0.149   1.  65.   0.21    8
 19 25 35.826      -0.208   1.  65.  -0.16    9
 19 25 54.326      -0.047   1.  64.  -0.01   10
 19 26  7.576      -0.152   1.  64.  -0.12   11
 19 26 38.326      -0.185   1.  63.  -0.18   12
 19 26 44.576      -0.140   1.  63.  -0.14   13
 19 27  0.325      -0.122   1.  63.  -0.14   14
 19 27 13.325       0.414   1.  62.   0.39   15
 19 28 35.575      -0.025   1.  59.  -0.11   16
*     7834        7603901
*    81  9  7    19 22 12.828
*    16 POINTS   16 ACCEPTED     0 REJECTED
*   RANGE  NOISE =    0.235 RMS =    0.220
*   TIME  OFFSET =     -0.265 +OR-    0.193 MSEC
*   RANGE OFFSET =      0.196 +OR-    0.112 METER
                                     SIGMA
```